Parasitology
December 2022, Volume 149, Issue 14, Pages 1976-1984
https://doi.org/10.1017/S0031182022001299
https://archimer.ifremer.fr/doc/00795/90747/

Unravelling the trophic interaction between a parasitic barnacle (*Anelasma squalicola*) and its host Southern lanternshark (*Etmopterus granulosus*) using stable isotopes

Sabadel A. J. M. [1, *], Cresson Pierre [2], Finucci B. [3], Bennett J. [1]

[1] Department of Zoology, University of Otago, PO Box 56, Dunedin 9045, New Zealand
[2] IFREMER, Channel and North Sea Fisheries Research Unit, 150 Quai Gambetta, BP 699, 62 321 Boulogne sur Mer, France
[3] National Institute of Water and Atmospheric Research (NIWA), 301 Evans Bay Parade, Hataitai, Wellington 6021, New Zealand

* Corresponding author : A. J. M. Sabadel, email address : amandine.sabadel@otago.ac.nz

Abstract :

The parasitic barnacle, Anelasma squalicola, is a rare and evolutionary fascinating organism. Unlike most other filter-feeding barnacles, A. squalicola has evolved the capability to uptake nutrient from its host, exclusively parasitizing deepwater sharks of the families Etmopteridae and Pentanchidae. The physiological mechanisms involved in the uptake of nutrients from its host are not yet known. Using stable isotopes and elemental compositions, we followed the fate of nitrogen, carbon and sulphur through various tissues of A. squalicola and its host, the Southern lanternshark Etmopterus granulosus, to better understand the trophic relationship between parasite and host. Like most marine parasites, A. squalicola is lipid-rich and clear differences were found in the stable isotope ratios between barnacle organs. It is evident that the deployment of a system of 'rootlets', which merge with host tissues, allows A. squalicola to draw nutrients from its host. Through this system, proteins are then rerouted to the exterior structural tissues of A. squalicola while lipids are used for maintenance and egg synthesis. The nutrient requirement of A. squalicola was found to change from protein-rich to lipid-rich between its early development stage and its definitive size.

Graphical abstract

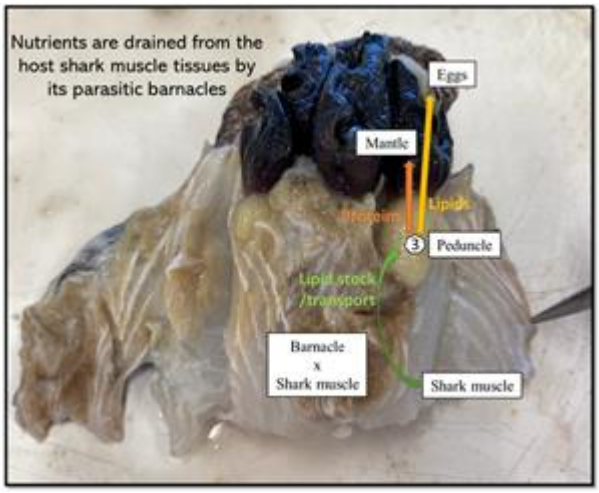

Keywords : Deepwater, food web, host–parasite, New Zealand, nitrogen, parasite, shark, stable isotopes, trophic position

Key Findings

- *Anelasma squalicola* has lipid-rich and protein-rich tissues.
- *A. squalicola* deploys "rootlets" that merge with shark tissue and enables drawing of host metabolites.
- The nutrient requirements of *A. squalicola* change from proteins to lipids with time.
- Fully developed *A. squalicola* reroute a large portion of lipids to produce their eggs.

Introduction

Evolutionary transitions to parasitism are very common in nature. Weinstein and Kuris (2016) estimated that parasitism has independently evolved over 200 times on the tree of life. One unique and fascinating transition involves the barnacle *Anelasma squalicola* Darwin, 1852 (Family Zevina 1980; https://www.marinespecies.org/aphia.php?p=taxdetails&id=106054), which infects deepwater sharks of the Etmopteridae and Pentanchidae families (Rees *et al.*, 2019). This barnacle is known to have a wide host and geographic distribution (Newman & Foster, 1987). Although *A. squalicola* is relatively uncommon in nature (Rees *et al.*, 2019), it can reach prevalence as high as 7% (calculated from Yano and Musick (2000)). Sharks can host between one and four barnacles embedded in tissues throughout the body, including the head, mouth, fins, abdomen, claspers and cloaca (Yano & Musick, 2000). *Anelasma squalicola* is suspected to have detrimental impacts on the health of their host, and the site of attachment is important for assessing the impact to host from damages caused by the parasite *e.g.,* when *A. squalicola* attaches on tissue around the gonads, they can retard the development of reproductive organs and thus, impact fecundity (Hickling, 1963; Yano & Musick, 2000).

Unsurprisingly, *A. squalicola*'s life cycle is not well-documented. Frost (1928) first reported a free-living nauplius stage, of which he stated that the morphology of *A. squalicola* strongly contrasts the morphology of filter-feeding barnacle nauplius. Presumably, a free-living

cypris stage exists, and then larvae somehow adhere themselves to their shark hosts and develop into their adult forms. Once attached, *A. squalicola* burrows into the flesh of its host by deploying a system of rootlets that will also be used to acquire nutrients from the host (Hickling, 1963; Long & Waggoner, 1993). Once settled, the barnacle can grow to maturation quite rapidly (Ommundsen *et al.*, 2016).

Only recently was *A. squalicola* confirmed as a true parasite, primarily because parasitism has only evolved a few times in the history of barnacle species (Cirripedia: Thoracica) (Ommundsen *et al.*, 2016). Other vertebrates, such as whales, sea snakes and turtles are commonly infected with suspension feeding phoresy barnacles. However, of the over one thousand species of stalked and acorn cirripeds, *A. squalicola* is the only non-epibiotic suspension feeder that feeds off the tissue of a vertebrate host (Ommundsen *et al.*, 2016). The supporting evidence for determining that *A. squalicola* has a parasitic feeding mode was that their alimentary tracts were void of food items, with their mouth parts reduced and appeared functionally redundant. This hypothesis was also confirmed through stable isotope analyses conducted on barnacles' mantle tissues and compared to their filter-feeding organs (Ommundsen *et al.*, 2016). Results indicated that compared to filter-feeding barnacles, *A. squalicola* had different stable isotope values, confirming the impossibility for *A. squalicola* to be feeding on surrounding particulate organic matter, and thus, only leaving the option of a parasitic lifestyle (Ommundsen et al. 2016). However, these results could have been tainted by the isotopic gradient usually observed between onshore shallow settings, where the filter-feeding barnacles were collected, and offshore deepwater settings, where the host sharks were caught. Furthermore, stable isotope analyses on the host muscle tissues were not conclusive as the "predator-prey" framework used in stable isotope ecology does not suit parasite-host interactions (Sabadel *et al.*, 2019; Thieltges *et al.*, 2019; Riekenberg *et al.*, 2020).

Stable isotopes ratios of carbon and nitrogen, and more recently of sulphur ($\delta^{13}C$, $\delta^{15}N$ and $\delta^{34}S$, respectively) have been widely used in ecology (Connolly *et al.*, 2004; Fry, 2006). They represent a powerful tool to understand the trophic relationship between a consumer and its food source. Indeed, carbon isotopic ratios do not vary considerably with each trophic level (~1‰), allowing the use of this element as a tracer of organic matter source (Post, 2002; Fry, 2006). Moreover, the relative depletion in $\delta^{13}C$ values is correlated with the presence of lipids, an important food resource for marine parasites (Sabadel & MacLeod, 2022). Similarly, $\delta^{34}S$ values, mainly represented by two amino acid, cysteine and methionine, in organic tissues show little change with trophic transfer (Peterson *et al.*, 1985; Krouse, 1991). On the contrary, nitrogen is gradually enriched through trophic transfer (~3.4‰), leading to high $\delta^{15}N$ values at high trophic levels (Post, 2002; Layman *et al.*, 2012), and allows for inferences of trophic position for a given species.

The stable isotope framework has been fine-tuned over decades to study predator-prey interactions; and more recently, this technique has also been increasingly utilized to help understand the trophic ecology of parasites (Sabadel *et al.*, 2016, 2019; Kanaya *et al.*, 2019; Sures *et al.*, 2019; Thieltges *et al.*, 2019; Kamiya *et al.*, 2020; Sánchez Barranco *et al.*, 2020; Taccardi *et al.*, 2020). The ability to select macromolecules from their host (while predators consume their whole prey) may explain the odd isotopic fractionation factors usually reported for parasites and is consistent with the hypothesis of a functional optimisation of parasites (Gilbert *et al.*, 2020; Riekenberg *et al.*, 2020). These recent findings call for more research into the application of stable isotope in parasitology.

The unique evolutionarily parasitic lifestyle of *A. squalicola* provides an ideal opportunity to use stable isotopes to understand the physiological mechanisms behind its feeding behaviour. Here, building on Ommundsen et al.'s (2016) work, we investigate the relationship between *A. squalicola* and its host, a deepwater Southern lanternshark (or Baxter's dogfish) *Etmopterus*

granulosus (Günther, 1880) using stable isotopes and elemental composition of carbon, nitrogen and, for the first time, sulphur, of various parasite and host tissues. We hypothesise that *A. squalicola* depletes its host of lipids, using them as a source of energy to support itself and the next generation parasitic barnacles. This study provides a pertinent example of the functional transformation associated with the evolution from a free-living filter-feeding life to a parasitic one.

Materials and methods

Collection of specimens

Specimens (host and parasite) were obtained during a fisheries independent research trawl survey conducted by the National Institute of Water and Atmospheric Research (NIWA), on board RV *Tangaroa* on Chatham Rise in January 2022 (TAN2201). Trawl surveys were stratified-random with resulting sampling strata defined by location and depth, and fishing occurred on trawlable fishing grounds. Sharks were measured for total length (TL, cm) and visually inspected for signs of parasite infections. Sharks confirmed to have barnacle infections were kept whole, frozen at sea, and brought back to the laboratory for analyses. In total, eight sharks were obtained for this study, representing 22 parasitic barnacles (Figure 1). Specimens were obtained from depths between 707 to 1261 m depth.

Shark and barnacle dissections

In the laboratory, sharks were defrosted and their barnacles and approximately 2 – 3 cm of surrounding host tissue were dissected to for stable isotope analysis. A total of 10 infection sites were identified, with two of the eight sharks infected in two separate locations. Each site contained either one (n = 1 site), two (n = 7 sites), three (n = 1 site) or four (n = 1 site) barnacles embedded together. For the host shark, 'healthy' muscle tissue was collected, close to each barnacle's sites, but beyond the reach of the rootlets (n = 22) (Figure 2A). For two of the sharks,

we also collected tissues that were clearly impacted by the presence of the barnacle. This tissue was labelled as 'unhealthy' (Figure 2A). For each barnacle, we isolated the following tissues: mantle (n = 22), mouth + cirri + penis (MCP, n = 21), rootlets (n = 22), peduncle (n = 22), and eggs (n = 12) (Figure 2B). All tissues were placed in individual Eppendorf tubes, and dried in an oven at 60 ^{o}C for at least 48 hours. We used the dried weight of the entire mantle as a proxy for barnacle size/age and categorised all individuals in one of the following size classes: Small < 50 mg, Medium 50 mg < weight < 100 mg, and Large > 100 mg.

Bulk stable isotope measurements

Stable isotope ratios of shark and barnacle tissues were measured at the Isotrace Lab in Dunedin, New Zealand. For each sample, approximately 0.8 mg of dried material was packed into a tin capsule and folded prior to stable isotope measurements. None of the samples were lipid-extracted so that the lipids impact on the δ^{13}C values was captured, as these were expected to be an important food resource to parasites. Values of δ^{15}N, δ^{13}C and δ^{34}S, along with the elemental compositions of carbon, nitrogen, and sulphur, were measured on an EA Isolink CNSOH coupled with a Delta V Advantage Isotopic Ratio Mass Spectrometer (Thermo Fisher). The stable isotope values are reported as: $\delta X = [(R_{sample}/R_{standard}) - 1] \times 1000$ where X is the element ^{13}C, ^{15}N or ^{34}S, and R is the corresponding isotope ratio ^{13}C/^{12}C, ^{15}N/^{14}N or ^{34}S/^{32}S, respectively. The standards used to calibrate the δ values were Vienna Peedee Belemnite (VPDB) for carbon, atmospheric N_2 for nitrogen, or Canyon Diablo troilite (CDT) for sulphur. The samples were standardized to international isotope reference materials G01, a mix of USGS40 and IAEA-S1 (δ^{15}N = -4.52‰, δ^{13}C = -26.39‰ and δ^{34}S = -0.30‰) and G02, a mix of USGS41 and IAEA-S2 (δ^{15}N = 47.55‰, δ^{13}C = 36.55‰ and δ^{34}S = 22.62‰). The quality control was conducted by applying an in-house laboratory control material, Keratin Internal Standard (δ^{15}N = 8.91‰, δ^{13}C = -21.14‰ and δ^{34}S = 13.08‰). Instrument precision was 0.05‰ for δ^{15}N values, 0.07‰ for δ^{13}C and 0.60‰ for δ^{34}S.

The specific case of the barnacles in the eye

One shark (shark no. 11) had two small barnacles embedded in its right eye. The barnacles appeared to embed in the vitreous of the eye and penetrate the cartilage behind with their rootlets to access muscle behind the cartilage (Figure 3A). We took this opportunity to investigate if *A. squalicola* fed on the tissues at the site of infection (i.e., the eye), or beyond site of infection where the rootlets are located (i.e., the muscle behind the eye cartilage). We used the 'protein tissues' (average values of the mantle, the rootlets, the inner mantle and the MCP tissues; Figure 3B) of all barnacles from this study (except those of shark no. 11) and estimated the differences (Δ) in stable isotopes values and elemental composition between barnacles and shark 'healthy' muscle tissues (Figure 3C), *e.g.* $\Delta^{15}N_{Parasite\text{-}Host}$ ('healthy' muscle) = $\delta^{15}N_{Parasite}$ ('protein tissues') - $\delta^{15}N_{Host}$ ('healthy' muscle). Differences were calculated for all barnacle-shark pairs excluding shark no. 11, then compared to the barnacles from shark no.11 vs the host eye tissues and vs the host muscle behind the eye cartilage.

Statistical analyses and parameters

The elemental C/N ratio is commonly used a proxy for lipid-rich vs protein-rich tissues, with a high ratio indicating the former and a low ratio the latter. Differences in isotopic and elemental content were compared by ANOVA, followed by Tukey post-hoc tests. Correlation between stable isotope values, elemental compositions, and biotic and abiotic parameters (shark length, latitude, and longitude) were estimated using Pearson correlation coefficient. All statistical analyses were run using R version 4.1.2 and the packages *multcomp* and *PeformanceAnalytics* (Hothorn *et al.*, 2008; Peterson & Carl, 2020; R Core Team, 2020).

Results

Stable isotope values and elemental compositions of the host shark

Of the 439 *E. granulosus* sampled during the TAN2201 voyage, 18 were found to be infected with *A. squalicola* (4% infection prevalence). Eight of these sharks were investigated in this study, covering six locations on the Chatham Rise, New Zealand (Figure 1). Of these, sampled sharks, there were two females and six males, measuring between 38 and 71 cm total length.

The 'healthy' muscle tissues of shark hosts had $\delta^{15}N$ values ranging from 9.6 to 14.0‰ (avg. 12.0 ±1.3‰), $\delta^{13}C$ values from -19.6 to -17.6 ‰ (avg. -18.7±0.8‰) and $\delta^{34}S$ from 19.6 to 21.2‰ (avg. 20.4±0.8‰) (Table 1 and Sd1). Further, $\delta^{13}C$ values of host 'healthy' muscle tissues were significantly and positively correlated with latitude (Pearson's $\rho = 0.88$, $p << 0.001$) and longitude ($\rho = 0.90$, $p << 0.001$) (Supplement Figure S1), while $\delta^{15}N$ and $\delta^{34}S$ values of the same tissue only correlated with longitude: positively ($\rho = 0.81$, $p < 0.001$) and negatively ($\rho = -0.82$, $p < 0.001$), respectively. We compared stable isotopes values of the 'healthy' and the 'unhealthy' shark muscle and found that the 'unhealthy' shark tissues exhibited lower $\delta^{15}N$ and $\delta^{13}C$, but slightly higher $\delta^{34}S$ values (Table S1). Additionally, 'unhealthy' tissues on average contained less nitrogen and slightly more carbon, thus increasing the C/N ratio, which is usually indicative of lipid-rich tissues. Percentage of sulphur was equivalent between 'healthy' and 'unhealthy' tissues (Table S1).

Stable isotope values and elemental compositions of parasitic barnacles

The average values for stable isotopes and elemental compositions of *A. squalicola* are reported in Table 1. All data for the various barnacle tissues of individual organisms can be found in the Supplement data (Tables Sd 2-9). There were no significant differences ($p > 0.05$) between the mantle, the rootlets, the inner mantle, and the MCP for stable isotope values, elemental compositions, or C/N ratios (see Pearson's correlations and post hoc tests in Table S2). Additionally, the C/N ratios of these four tissues are relatively low (avg. 3.6±0.6 to 4.1±0.9) in comparison to the other selected parts of the parasite ($C/N_{Peduncle}$ = 6.6±3.5 and C/N_{Eggs} =

10.9±1.1), thus reflecting protein-rich tissues. As such, the mantle, the rootlets, the inner mantle, and the MCP were combined into a 'protein tissues' category.

Subsequently, based on the average values of each barnacle tissues (Table 1), the highest δ^{15}N values were the peduncles (avg. 11.7±1.6‰) and the lowest were the protein tissues (avg. 10.6±1.4‰), although these were not significantly different (Table S2). Conversely, for δ^{13}C the highest values were the 'protein tissues' (avg. -19.0±0.6‰), while the lowest were the eggs (avg. -22.1±0.5‰), where a difference was found between the two tissues (Table S2). For δ^{34}S the highest values were the 'protein tissues' (avg. 21.3±0.5‰) and the lowest were the eggs (avg. 19.8±0.8‰).

The barnacles' mantle dried weights were used as a proxy for the parasites size. These mantle weights ranged from 4.85 to 226.67 mg, covering a wide range of sizes. Within the 'protein tissues', the size (mantle weight) of *A. squalicola* was strongly and negatively correlated with δ^{15}N values (ρ = -0.75, p <0.001; Figure S2), δ^{34}S values (ρ = -0.83, p <0.001; Figure S2) and %S (ρ = -0.69, p <0.05; Figure S2). Further, within the peduncle tissues, the size of *A. squalicola* was negatively correlated with %N (ρ = -0.78, p <0.001; Figure S3), and %S (ρ = -0.81, p <0.001; Figure S3), and positively correlated with %C (ρ = 0.83, p <0.001; Figure S3) and with the C/N ratio (ρ = 0.79, p <0.001; Figure S3). Additionally, the barnacle size was negatively correlated with both the peduncle's δ^{13}C (ρ = -0.81, p <0.05; Figure S3) and δ^{34}S values (ρ = -0.87, p <0.05; Figure S3).

The effect of the number of barnacles per infection site (Figure S4) appeared to show differences in most stable isotope values and elemental compositions for one and three barnacles in comparison with clusters of two and four individuals. These observed differences were likely due to a size effect because these barnacles were relatively small compared to the ones that occupied sites as groups of two or four (Table Sd2-7 for barnacles' sizes/dried mantle weights).

The specific case of the barnacles in the eye

For shark no.11 (i.e., the only shark exhibiting barnacles settled in the eye; Figure 3A), isotopic or elemental differences between *A. squalicola* and either the eye, or the muscle behind the eye have been plotted in Figure 3C. Average difference between 'muscle-embedded' barnacles (i.e., all other barnacles excluding those of shark no. 11) and the 'healthy' muscles tissues of their respective host was used as a reference. This comparison highlighted that the differences between the barnacle from shark no. 11 and the eye were closer to the reference for all carbon and sulphur-related descriptors, including the C/N ratio, but were only holding for %N and not for δ^{15}N values (Figure 3C).

Discussion

We hypothesised that the *A. squalicola* depletes their shark host of lipids and as such, expected the 'unhealthy' shark tissue to be lipid-drained by the passive-feeding parasites. However, stable isotope values and elemental compositions indicated that the 'unhealthy' shark tissues are in fact, a mixture of barnacle rootlets and shark muscle. Here the rootlets transport nutrients (i.e., majority of lipids and few proteins) from the surrounding 'healthy' host muscle tissue to their peduncle, before nutrients are then redistributed to the 'protein tissues' and egg stock. This is evidenced by our findings below.

Unravelling the feeding mechanism of Anelasma squalicola

Higher lipid content than in 'healthy' shark muscle tissues were observed in all parasite organs analysed (see %C and C/N ratios in Table 1). This was even more marked in the barnacle's peduncle and egg tissues. In fact, with lipids exhibiting lower δ^{13}C values than other carbon-containing molecules, the observed depletion gradient along with an increasing carbon content between host and parasite is pointing to a clear path of lipid transport: from 'healthy' to 'unhealthy' shark muscle tissues, then to the egg stocks via the peduncle. In parallel, the

255 'protein tissues', representing the structure of the barnacle, displayed a similar $\delta^{13}C$ values and
256 carbon content than that of the 'unhealthy' shark muscle tissues and a rather low C/N ratio
257 typical of high protein content. Interestingly, while nitrogen content was statistically different
258 across the various barnacle organs and lower compared to the shark muscle tissues, the $\delta^{15}N$
259 and $\delta^{34}S$ values, and sulphur content stayed relatively constants. This could be interpreted as a
260 second nutrient pathway from host to parasite, whereby proteins are rerouted to the 'protein
261 tissues' after being first absorbed and possibly enzymatically reworked in the 'unhealthy'
262 muscle tissues. We illustrated this proposed mechanism of the redistribution of host nutrients
263 to different barnacle organs in Figure 4.

264 Further, Ommundsen *et al.* (2016) suggested that the high lipid content of *A. squalicola*
265 may result from the uptake of hosts' interstitial fluid, which is also rich in lipids. If true, and
266 considering our findings, there could be two possible scenarios: 1) the intestinal fluid contains
267 depleted host metabolites, and/or 2) the parasite can select the metabolites to incorporate within
268 its own tissues and chooses the most energy efficient (light isotopes-containing ones).
269 However, neither the potential enzymatic reworking nor the fractionation during these
270 metabolite uptakes by the parasite can be perceived by bulk stable isotope analysis, and
271 therefore it is not possible to distinguish between the scenarios and fully characterise the uptake
272 mechanisms. As such, this framework would largely benefit from further investigation into the
273 exact routing of proteins and lipids, *e.g.,* by analysing amino acid or fatty acid compositions of
274 the different tissues. This would allow confirming that protein and lipids demands – and
275 subsequent host to parasite nutrient fluxes – do change with growth or reproduction status of
276 the barnacle. In addition, compound-specific stable isotopic analysis (CSIA) of amino acids
277 could also be powerful to ascertain the effect of metabolism on parasite's isotopic ratio and
278 could help tease apart enzymatic activities (Sabadel *et al.*, 2019; Riekenberg *et al.*, 2021), while
279 CSIA of fatty acid (e.g., polysaturated long chain fatty acids) could shed light on the routing

of lipid from host to parasite (Twining *et al.*, 2020). Nevertheless, these results are aligned with other studies looking at 'absorptive' parasites such as acanthocephalan (Nachev *et al.*, 2017) or cestodes (Power & Klein, 2004; Finn *et al.*, 2022), challenging the classic framework of predator-prey relationships (i.e., $\delta^{15}N$ enrichment from prey to predator) (Thieltges *et al.*, 2019; Kamiya *et al.*, 2020; Sabadel & MacLeod, 2022).

The correlations of each measured variable (stable isotopes values and elemental compositions) with barnacle sizes could be indicative of a metabolic shift leading to different nutrient requirements between developing and fully-grown organisms. Indeed, it seems that in the early stages of their development, *A. squalicola* requires more protein and less lipids than later in its life, as evidenced by the lower %N, %S, $\delta^{13}C$, $\delta^{34}S$ and the higher %C, C/N ratio in larger individuals. As such, on one hand, small barnacles require more proteins to grow their structure and less lipids as they are not yet fully reproductively active. Adult barnacles on the other hand, swap this nutrition style for a lipid rich diet with relatively less proteins. Lipids dynamics was largely demonstrated as a major driver of host-parasites exchanges, by example for nematodes (Strømnes & Andersen, 2003; Strømnes, 2014; Mille *et al.*, 2020). Indeed, egg synthesis in marine environments consists mostly of an accumulation of lipids, which will represent future reserves of energy supporting the early development of newly hatched larvae (e.g., Kolodzey *et al.* (2021)) . The main function of an adult parasite, along with its own maintenance, is to produce and emit eggs. As such, functional simplification must have driven their ability to uptake lipid from their host in order to fuel the eggs' reserves. Results obtained here seem to demonstrate that the important role of lipids in adult barnacles can be generalized to other parasitic groups. However, other parasite tissues such as the 'protein tissues' also indicate some reliance on proteins. Further, the high variation in stable isotope values and elemental composition of the peduncle tends to confirm that it is the only feeding organ present, and as such, the nutrients stored in it might change depending on the barnacle's requirements

(*e.g.* depending on its spawning status). The parasite may divert metabolic resources that are required for normal reproductive development in the hosts, which live in deep habitats where energy may be in short supply (Yano & Musick, 2000).

Interestingly, while the $\delta^{15}N$ values from this study matched well the results from Ommundsen *et al.* (2016) for similar tissues (i.e., shark muscle and barnacle mantle), $\delta^{13}C$ values yield the opposite trend: authors found the barnacle to be enriched in $\delta^{13}C$, which would emphasise the use of protein for the 'protein tissues' rather than a combination of protein and lipids. However, it could not be determined whether the barnacle samples had been lipid-extracted prior to stable isotope analysis, as this methodological point is not specified in Ommundsen et al. (2016). This would have indeed enriched the $\delta^{13}C$ values of the mantle tissues and represented non-lipid molecules. Extracting lipids from parasites or host tissues prior to stable isotope analyses may blur the pattern of organic matter transfer between host and parasites, as lipids are a key (and sometime the only) food resource of parasites. Moreover, lipid-extraction protocol has revealed a crucial step in the robust application of stable isotopes in trophic ecology. It is now applied routinely to assess predator-prey interactions, as several calibrations of the seminal protocol proposed by Post *et al.* (2007) allowed the generalisation of the method to different conditions (e.g. Kiljunen *et al.* (2006), Logan *et al.* (2008)). The possible methodological discrepancy observed here seems however to confirm again the need for a similar development of a dedicated theoretical and methodological framework, before being able to apply routinely stable isotopes to host-parasite interactions.

The specific case of the barnacles in the eye

Most of the barnacles collected for this study were found attached to the sharks' body (*e.g.* dorsal fin, pectoral fin, tail), or embedded within their claspers. One infection site was in the eye (Figure 3A). The close resemblance of the differences between the two barnacles and the shark eye tissue in the averaged values of all variables – whether stable isotope values or

elemental compositions – confirmed that *A. squalicola* likely feeds on the eye rather than on the muscle behind the cartilage of their host's head. Although the small sample size (n = 2) precludes from generalisation of the pattern observed, this could indicate that the "rootlets", which had pierced through the eye, might not be the mean *via* which *A. squalicola* is feeding, as previously suggested (Hickling, 1963; Long & Waggoner, 1993). Instead, they may only be used for anchoring the barnacle in this instance. In this scenario, the barnacles would be feeding on the shark by mixing the peduncle tissues (i.e., different type of rootlets) with the surrounding host muscle tissues, as indicated by the nature of the 'unhealthy' host muscle tissues. This assemblage of barnacle and shark tissues could then become a path for the parasite to channel nutrients, in the form of a fluid in which the peduncle is sitting. Variability of the peduncle stable isotope values and elemental compositions may support the hypothesis of reworking of obtained lipids (*e.g.* fatty acids) by the peduncle, prior to rerouting them to its eggs stock.

Other insights

Two *Anelasma squalicola* per infection site was by far the predominant occurrence. Yano and Musick (2000) reported that over 70% of all infection sites had two *A. squalicola*. This is supported by our data as seven of the 10 infections hosted two barnacle individuals. In the one case where a single barnacle attached to a shark, the individual was small (mantle dried weight < 50 mg) indicating it was probably an early infection. We also found occurrences of three and four barnacles per infection site. In the case of the three barnacles, while all small, two had similar sizes with a third much smaller, possibly indicating their various order of arrival. For the four barnacle infection, all individuals were large in size and were likely parasitising the shark for some time, as demonstrated by the relatively extensive amount of 'unhealthy' shark tissues, compared to other samples (*e.g.* Figure 2A infection compared to Figure 4). There were some differences between individual barnacles within infection sites, but there was no clear positive or negative trend that indicated size - and by extension age – was not the factor

355 influencing these differences. One possibility for this phenomenon could be that as barnacles
356 infect the same site, all the barnacles' rootlets intertwine into one common block of
357 barnacle/shark tissue, as indicated by the values of 'unhealthy' shark muscle tissue (Table 1
358 and S2). This could be advantageous or disadvantageous to individual barnacles depending on
359 their position within the cluster and their access to the nutrients/host metabolites.

360 The *E. granulosus* $\delta^{13}C$ values were strongly and positively correlated with latitude and
361 longitude, following the known $\delta^{13}C$ tropical-Antarctic (Graham & Bury, 2019) and the
362 onshore-offshore depletion gradients, respectively. These reflected differences in temperature
363 and the solubility of CO_2 as observed elsewhere (Goericke & Fry, 1994; Laws *et al.*, 1995;
364 Graham *et al.*, 2010; Trueman *et al.*, 2012) and are shown here for Chatham Rise. Stable
365 isotope spatial variations were also marginally observed positively for $\delta^{15}N$ and negatively for
366 $\delta^{34}S$ values across a latitudinal gradient. With stable isotopes representing time-integrated
367 information, this spatial relationship within shark tissues could indicate that these sharks
368 remain resident to a relatively small region, consistent with previous results obtained elsewhere
369 (Bird *et al.*, 2018). *Etmopterus granulosus* has a strong affinity to seamount communities
370 (Finucci *et al.*, 2018), and although the species has widespread distribution across the Southern
371 Hemisphere (Straube *et al.*, 2011), any finer scale population structure is currently unknown.
372 Further, the relatively high $\delta^{34}S$ values obtained for *E. granulosus* seem to indicate offshore
373 pelagic rather than inshore and/or benthic feeding for these sharks (Connolly *et al.*, 2004). This
374 finding is however in contradiction with results from visual diet studies (Dunn *et al.*, 2013) and
375 warrants further investigation.

376 Interestingly, the $\delta^{13}C$ gradients observed in the sharks' 'healthy' muscle tissues was also
377 detectable within the barnacles but only in the 'protein tissues', and across a longitudinal
378 gradient. This lack of gradients could underscore the complex metabolic processes happening
379 within the barnacle, as neither the peduncle nor the egg stock covaried with either latitude or

longitude. This finding may be attributed to the parasite's absorptive feeding mode which here again defies the classic predator-prey interactions as the $\delta^{13}C$ values showed little to no fractionation. In addition, organs such at the mouth and cirri (as main parts of the MCP) are structures without function, and may thus have limited metabolically activity since they are no longer used for food capture (Rees *et al.*, 2014).

Conclusion

In this study we unravel the importance of lipids as a driver of the interaction between the parasitic barnacle *A. squalicola* and its host shark *E. granulosus*. Using stable isotopes, we tracked the flow of N, C and S, and ultimately protein and lipids from host to parasite by passive feeding i.e., absorption of selected nutrients/host metabolites. This is similar to other passive feeding marine parasites (Sabadel & MacLeod, 2022). *Anelasma squalicola* is a representative of just one independent evolutionary transition of the over 200 currently reported in the history of metazoans. Although independent, this particular transition has convergently evolved similar mechanisms to other parasites for which to obtain nutrients. We propose a mechanism whereby the barnacle tissue fusion with the shark muscle tissues, thus creating a mix of parasite and shark tissues that potentially expands in response to increased nutrients demands for parasite *e.g.,* as the number of barnacle in a cluster increases and with size and/or maturity of an individual parasite. Once the nutrients have reached the peduncle, proteins are rerouted in the 'protein tissues', especially in the initial growth spurt of the barnacles, while the lipids are mostly channelled to generate the eggs and secure the next generation. Further research could include fatty acid profiling and both CSIA of fatty acids and amino acids to understand which compounds are absorbed by the barnacle from its host shark. Investigating the relatedness of barnacles that infect the same site would provide great insight into the life cycle of this mysterious parasite.

Supplementary material (heading only required if your paper contains supplementary material)

These are materials that are not necessary to replicate the findings of the article but which add depth or context to the main paper. Such files are usually made available on the Cambridge University Press platform alongside the article.

Data (heading only required if data is available elsewhere)

Data Availability Statements are brief statements telling readers how they can access the data and other materials that would be necessary to replicate the findings of an article, in the interests of research transparency.

Acknowledgements (optional)

Special thank you to Robert Poulin for giving us access to his laboratory resources. This project was made possible by the cooperation and assistance in sample collection provided by the staff and crew of the RV *Tangaroa.*

Author Contribution (optional)

AJMS, BF and JB formulated the core questions of the article. BF collected the shark samples. JB dissected the shark and barnacles' various tissues. AJMS prepared the samples for stable isotope measurements. PC ran the statistics. AJMS and PC analysed and discussed the results. AJMS wrote the manuscript with inputs from PC, BF and JB. All authors gave final approval for publication.

Financial Support (mandatory)

We thank the New Zealand Royal Society Marsden Fund (19-UOO-212) for supporting this research and AJMS's salary.

Conflicts of Interest (mandatory)

The authors declare there are no conflicts of interest.

Ethical Standards (mandatory)

Not applicable.

References

Bird, C. S., Veríssimo, A., Magozzi, S., Abrantes, K. G., Aguilar, A., Al-Reasi, H., Barnett, A., Bethea, D. M., Biais, G., Borrell, A., Bouchoucha, M., Boyle, M., Brooks, E. J., Brunnschweiler, J., Bustamante, P., Carlisle, A., Catarino, D., Caut, S., Cherel, Y., Chouvelon, T., Churchill, D., Ciancio, J., Claes, J., Colaço, A., Courtney, D. L., Cresson, P., Daly, R., de Necker, L., Endo, T., Figueiredo, I., Frisch, A. J., Hansen, J. H., Heithaus, M., Hussey, N. E., Iitembu, J., Juanes, F., Kinney, M. J., Kiszka, J. J., Klarian, S. A., Kopp, D., Leaf, R., Li, Y., Lorrain, A., Madigan, D. J., Maljković, A., Malpica-Cruz, L., Matich, P., Meekan, M. G., Ménard, F., Menezes, G. M., Munroe, S. E. M., Newman, M. C., Papastamatiou, Y. P., Pethybridge, H., Plumlee, J. D., Polo-Silva, C., Quaeck-Davies, K., Raoult, V., Reum, J., Torres-Rojas, Y. E., Shiffman, D. S., Shipley, O. N., Speed, C. W., Staudinger, M. D., Teffer, A. K., Tilley, A., Valls, M., Vaudo, J. J., Wai, T.-C., Wells, R. J. D., Wyatt, A. S. J., Yool, A. and Trueman, C. N. (2018). A global perspective on the trophic geography of sharks. *Nature Ecology & Evolution,* **2**, 299-305. doi: 10.1038/s41559-017-0432-z.

Connolly, R. M., Guest, M. A., Melville, A. J. and Oakes, J. M. (2004). Sulfur stable isotopes separate producers in marine food-web analysis. *Oecologia,* **138**, 161-167. doi: 10.1007/s00442-003-1415-0.

Dunn, M. R., Stevens, D. W., Forman, J. S. and Connell, A. (2013). Trophic Interactions and Distribution of Some Squaliforme Sharks, Including New Diet Descriptions for Deania calcea and Squalus acanthias. *PLoS ONE,* **8**, e59938. doi: 10.1371/journal.pone.0059938.

Finn, K. J., Roberts, K. N. and Poesch, M. S. (2022). Cestode parasites are depleted in 15N relative to their fish hosts in northern Alberta, Canada. *Fisheries Research,* **248**, 106193. doi: https://doi.org/10.1016/j.fishres.2021.106193.

Finucci, B., Dunn, M. R., Jones, E. G. and Bartolino, H. e. V. (2018). Aggregations and associations in deep-sea chondrichthyans. *ICES Journal of Marine Science,* **75**, 1613-1626. doi: 10.1093/icesjms/fsy034.

Frost, W. F. (1928). The nauplius larva of *Anelasma squalicola* (Lovén). *Journal of the Marine Biological Association of the United Kingdom,* **15**, 125-128.

Fry, B. (2006). *Stable isotope ecology,* Springer-Verlag New York, New York.

Gilbert, B. M., Nachev, M., Jochmann, M. A., Schmidt, T. C., Köster, D., Sures, B. and Avenant-Oldewage, A. (2020). You are how you eat: differences in trophic position of two parasite species infecting a single host according to stable isotopes. *Parasitol Res,* **119**, 1393-1400. doi: 10.1007/s00436-020-06619-1.

Goericke, R. and Fry, B. (1994). Variations of marine plankton $\delta^{13}C$ with latitude, temperature, and dissolved CO_2 in the world ocean. *Global Biogeochemical Cycles,* **8**, 85-90. doi: https://doi.org/10.1029/93GB03272.

Graham, B. and Bury, S. J. (2019). *Marine isoscapes for trophic and animal movement studies in the southwest Pacific Ocean*.

Graham, B. S., Koch, P. L., Newsome, S. D., McMahon, K. W. and Aurioles, D. (2010). Using isoscapes to trace the movements and foraging behavior of top predators in oceanic ecosystems. In *Isoscapes: Understanding movement, pattern, and process on Earth through isotope mapping* (eds. West, J. B., Bowen, G. J., Dawson, T. E., and Tu, K. P.), pp. 299-318. Springer Netherlands, Dordrecht.

Hickling, C. F. (1963). On the small deep-sea shark *Etmopterus spinax* L., and its cirripede parasite *Anelasma squalicola* (Lovén). *Journal of the Linnean Society of London, Zoology,* **45**, 17-24. doi: https://doi.org/10.1111/j.1096-3642.1963.tb00484.x.

Hothorn, T., Bretz, F. and Westfall, P. (2008). Simultaneous inference in general parametric models. *Biom J,* **50**, 346-363. doi: 10.1002/bimj.200810425.

Kamiya, E., Urabe, M. and Okuda, N. (2020). Does atypical ^{15}N and ^{13}C enrichment in parasites result from isotope ratio variation of host tissues they are infected? *Limnology,* **21**, 139-149. doi: 10.1007/s10201-019-00596-w.

Kanaya, G., Solovyev, M. M., Shikano, S., Okano, J.-i., Ponomareva, N. M. and Yurlova, N. I. (2019). Application of stable isotopic analyses for fish host–parasite systems: an evaluation tool for parasite-mediated material flow in aquatic ecosystems. *Aquatic Ecology,* **53**, 217-232. doi: 10.1007/s10452-019-09684-6.

Kiljunen, M., Grey, J., Sinisalo, T., Harrod, C., Immonen, H. and Jones, R. I. (2006). A revised model for lipid-normalizing $\delta^{13}C$ values from aquatic organisms, with implications for isotope mixing models. *Journal of Applied Ecology,* **43**, 1213-1222. doi: https://doi.org/10.1111/j.1365-2664.2006.01224.x.

Kolodzey, S., Durante, L. M., Sabadel, A. J. M. and Wing, S. R. (2021). Larval quality and fecundity trade-offs are linked to the maternal environment in sea perch (Helicolenus percoides, Sebastidae). *Journal of Experimental Marine Biology and Ecology,* **537**, 151525. doi: https://doi.org/10.1016/j.jembe.2021.151525.

Krouse, H. R. (1991). *Stable isotopes: natural and anthropogenic sulphur in the environment,* John Wiley and Sons, United Kingdom.

Laws, E. A., Popp, B. N., Bidigare, R. R., Kennicutt, M. C. and Macko, S. A. (1995). Dependence of phytoplankton carbon isotopic composition on growth rate and (CO_2)aq: Theoretical considerations and experimental results. *Geochimica et Cosmochimica Acta,* **59**, 1131-1138. doi: https://doi.org/10.1016/0016-7037(95)00030-4.

Layman, C. A., Araujo, M. S., Boucek, R., Hammerschlag-Peyer, C. M., Harrison, E., Jud, Z. R., Matich, P., Rosenblatt, A. E., Vaudo, J. J., Yeager, L. A., Post, D. M. and Bearhop, S. (2012). Applying stable isotopes to examine food-web structure: an overview of analytical tools. *Biological Reviews,* **87**, 545-562. doi: https://doi.org/10.1111/j.1469-185X.2011.00208.x.

Logan, J. M., Jardine, T. D., Miller, T. J., Bunn, S. E., Cunjak, R. A. and Lutcavage, M. E. (2008). Lipid corrections in carbon and nitrogen stable isotope analyses: comparison of chemical extraction and modelling methods. *Journal of Animal Ecology,* **77**, 838-846. doi: https://doi.org/10.1111/j.1365-2656.2008.01394.x.

Long, D. J. and Waggoner, B. M. (1993). The ectoparasitic barnacle Anelasma (Cirripedia, Thoracica, Lepadomorpha) on the shark Centroscyllium nigrum (Chondrichthyes, Squalidae) from the Pacific sub-Antarctic. *Systematic Parasitology,* **26**, 133-136. doi: 10.1007/BF00009220.

Mille, T., Soulier, L., Caill-Milly, N., Cresson, P., Morandeau, G. and Monperrus, M. (2020). Differential micropollutants bioaccumulation in European hake and their parasites Anisakis sp. *Environ Pollut,* **265**, 115021. doi: 10.1016/j.envpol.2020.115021.

Nachev, M., Jochmann, M. A., Walter, F., Wolbert, J. B., Schulte, S. M., Schmidt, T. C. and Sures, B. (2017). Understanding trophic interactions in host-parasite associations using stable isotopes of carbon and nitrogen. *Parasites & Vectors,* **10**, 90. doi: 10.1186/s13071-017-2030-y.

Newman, W. A. and Foster, B. A. (1987). Southern-Hemisphere Endemism among the Barnacles - Explained in Part by Extinction of Northern Members of Amphitropical Taxa. *Bulletin of Marine Science,* **41**, 361-377.

Ommundsen, A., Noever, C. and Glenner, H. (2016). Caught in the act: phenotypic consequences of a recent shift in feeding strategy of the shark barnacle *Anelasma*

squalicola (Lovén, 1844). *Zoomorphology,* **135**, 51-65. doi: 10.1007/s00435-015-0296-1.

Peterson, B. G. and Carl, P. (2020). PerformanceAnalytics: Econometric Tools for Performance and Risk Analysis. . *R package version 2.0.4.*

Peterson, B. J., Howarth, R. W. and Garritt, R. H. (1985). Multiple stable isotopes used to trace the flow of organic matter in estuarine food webs. *Science,* **227**, 1361-1363. doi: 10.1126/science.227.4692.1361.

Post, D. M. (2002). Using stable isotopes to estimate trophic position: models, methods, and assumptions. *Ecology,* **83**, 703-718. doi: 10.1890/0012-9658(2002)083[0703:usitet]2.0.co;2.

Post, D. M., Layman, C. A., Arrington, D. A., Takimoto, G., Quattrochi, J. and Montaña, C. G. (2007). Getting to the Fat of the Matter: Models, Methods and Assumptions for Dealing with Lipids in Stable Isotope Analyses. *Oecologia,* **152**, 179-189.

Power, M. and Klein, G. (2004). Fish host-cestode parasite stable isotope enrichment patterns in marine, estuarine and freshwater fishes from Northern Canada. *Isotopes Environ Health Stud,* **40**, 257-266. doi: 10.1080/10256010410001678062.

R Core Team (2020). R: A Language and Environment for Statistical Computing [Internet]. R Foundation for Statistical Computing, Vienna, Austria. Available from: https://www.R-project.org.

Rees, D. J., Noever, C., Finucci, B., Schnabel, K., Leslie, R. E., Drewery, J., Theil Bergum, H. O., Dutilloy, A. and Glenner, H. (2019). De novo innovation allows shark parasitism and global expansion of the barnacle *Anelasma squalicola*. *Current Biology,* **29**, R562-R563. doi: https://doi.org/10.1016/j.cub.2019.04.053.

Rees, David J., Noever, C., Høeg, Jens T., Ommundsen, A. and Glenner, H. (2014). On the origin of a novel parasitic-feeding mode within suspension-feeding barnacles. *Current Biology,* **24**, 1429-1434. doi: https://doi.org/10.1016/j.cub.2014.05.030.

Riekenberg, P. M., Briand, M. J., Moléana, T., Sasal, P., van der Meer, M., Thieltges, D. W. and Letourneur, Y. (2020). Impacts of host phylogeny, feeding styles, and parasite attachment site on isotopic discrimination in helminths infecting coral reef fish hosts. *bioRxiv*, 2020.2005.2031.126110. doi: 10.1101/2020.05.31.126110.

Riekenberg, P. M., Joling, T., IJsseldijk, L. L., Waser, A. M., van der Meer, M. T. J. and Thieltges, D. W. (2021). Stable nitrogen isotope analysis of amino acids as a new tool to clarify complex parasite–host interactions within food webs. *Oikos,* **130**, 1650-1664. doi: https://doi.org/10.1111/oik.08450.

Sabadel, A. J. M. and MacLeod, C. D. (2022). Stable isotopes unravel the feeding mode–trophic position relationship in trematode parasites. *Journal of Animal Ecology,* **91**, 484-495. doi: https://doi.org/10.1111/1365-2656.13644.

Sabadel, A. J. M., Stumbo, A. D. and MacLeod, C. D. (2019). Stable isotope analysis: a neglected tool for placing parasites in food webs. *Journal of Helminthology,* **93**, 1-7. doi: 10.1017/S0022149X17001201.

Sabadel, A. J. M., Woodward, E. M. S., Van Hale, R. and Frew, R. D. (2016). Compound-specific isotope analysis of amino acids: a tool to unravel complex symbiotic trophic relationships. *Food Webs,* **6**, 9-18. doi: http://dx.doi.org/10.1016/j.fooweb.2015.12.003.

Sánchez Barranco, V., Van der Meer, M. T. J., Kagami, M., Van den Wyngaert, S., Van de Waal, D. B., Van Donk, E. and Gsell, A. S. (2020). Trophic position, elemental ratios and nitrogen transfer in a planktonic host–parasite–consumer food chain including a fungal parasite. *Oecologia*. doi: 10.1007/s00442-020-04721-w.

Straube, N., Kriwet, J. and Schliewen, U. K. (2011). Cryptic diversity and species assignment of large lantern sharks of the *Etmopterus spinax* clade from the Southern

Hemisphere (Squaliformes, Etmopteridae). *Zoologica Scripta,* **40**, 61-75. doi: https://doi.org/10.1111/j.1463-6409.2010.00455.x.

Strømnes, E. (2014). An in vitro study of lipid preference in whaleworm (*Anisakis simplex*, Nematoda, Ascaridoidea, Anisakidae) third-stage larvae. *Parasitology Research,* **113**, 1113-1118. doi: 10.1007/s00436-013-3748-x.

Strømnes, E. and Andersen, K. (2003). Growth of whaleworm (*Anisakis simplex*, Nematodes, Ascaridoidea, Anisakidae) third-stage larvae in paratenic fish hosts. *Parasitology Research,* **89**, 335-341. doi: 10.1007/s00436-002-0756-7.

Sures, B., Nachev, M., Gilbert, B. M., Dos Santos, Q. M., Jochmann, M. A., Köster, D., Schmidt, T. C. and Avenant-Oldewage, A. (2019). The monogenean Paradiplozoon ichthyoxanthon behaves like a micropredator on two of its hosts, as indicated by stable isotopes. *Journal of Helminthology,* **93**, 71-75. doi: 10.1017/S0022149X17001195.

Taccardi, E. Y., Bricknell, I. R. and Byron, C. J. (2020). Stable isotopes reveal contrasting trophic dynamics between host–parasite relationships: a case study of Atlantic salmon (Salmo salar) and parasitic lice (Lepeophtheirus salmonis and Argulus foliaceus). *Journal of Fish Biology,* **n/a**. doi: 10.1111/jfb.14546.

Thieltges, D. W., Goedknegt, M. A., O'Dwyer, K., Senior, A. M. and Kamiya, T. (2019). Parasites and stable isotopes: a comparative analysis of isotopic discrimination in parasitic trophic interactions. *Oikos*. doi: 10.1111/oik.06086.

Trueman, C. N., MacKenzie, K. M. and Palmer, M. R. (2012). Identifying migrations in marine fishes through stable-isotope analysis. *Journal of Fish Biology,* **81**, 826-847. doi: 10.1111/j.1095-8649.2012.03361.x.

Twining, C. W., Taipale, S. J., Ruess, L., Bec, A., Martin-Creuzburg, D. and Kainz, M. J. (2020). Stable isotopes of fatty acids: current and future perspectives for advancing trophic ecology. *Philosophical Transactions of the Royal Society B: Biological Sciences,* **375**, 20190641. doi: doi:10.1098/rstb.2019.0641.

Weinstein, S. B. and Kuris, A. M. (2016). Independent origins of parasitism in Animalia. *Biol Lett,* **12**. doi: 10.1098/rsbl.2016.0324.

Yano, K. and Musick, J. A. (2000). The Effect of the Mesoparasitic Barnacle Anelasma on the Development of Reproductive Organs of Deep-sea Squaloid Sharks, Centroscyllium and Etmopterus. *Environmental Biology of Fishes,* **59**, 329-339. doi: 10.1023/A:1007649227422.

Appendix (optional)

Any Appendices should be placed after References

Figures legends

Figure 1. Map depicting the locations where *Etmopterus granulosus* infected with *Anelasma squalicola* were collected on Chatham Rise, New Zealand in January 2022. The number of parasitic barnacles and their site of infection on each host shark is indicated by the green ovals.

Figure 2. *Anelasma squalicola in situ* on *Etmopterus granulosus*. A) Pre-dissection photo of *A. squalicola* infecting *E. granulosus* (left) and partially dissected *A. squalicola* showing 'unhealthy' host tissue infested with *A. squalicola* rootlets, Pd, and healthy host tissue (H) (right). B) Two parasitic barnacles (varying in size) illustrating tissues taken for stable isotope analyses. These include mouth, cirri and penis (MCP), eggs (Egg), mantle (M), peduncle (Pd), and rootlets (R). Not represented is the inner mantle, a soft tissue found within the mantle. Scale bars represent 1cm.

Figure 3. A) *A. squalicola in situ* of the right eye of *E. granulosus* whereby rootlets appear to have penetrated host cartilage for access to host muscle in the centre of the shark head. B) Visual characterisation of *A. squalicola* identified as either protein-rich (purple) or lipid- rich (pink) tissues. C) Stable isotope values and elemental compositions differences between parasite and host tissues. The difference between all barnacle 'protein tissues' (mean of all barnacles except individuals on shark no. 11 and their matching shark 'healthy' muscle tissues; green); the difference between shark no. 11's barnacle 'protein tissues' and the eye tissue of the shark (grey); and the difference between shark no. 11 barnacle's 'protein tissues' and the 'healthy' shark muscle tissue (yellow).

Figure 4. Proposed physiological mechanisms behind parasitic barnacle feeding. (1) 'Healthy' shark muscle tissue, (2) 'unhealthy' shark tissue, (3) one of the barnacle's peduncle, (4) the

645 same barnacle's protein tissues and (5) its egg stock. Green arrow represents a transfer of lipids
646 and proteins *via* the barnacle's rootlets, orange arrow represents a transfer of proteins for
647 maintenance and yellow arrow represents a transfer of lipids to the next generation.

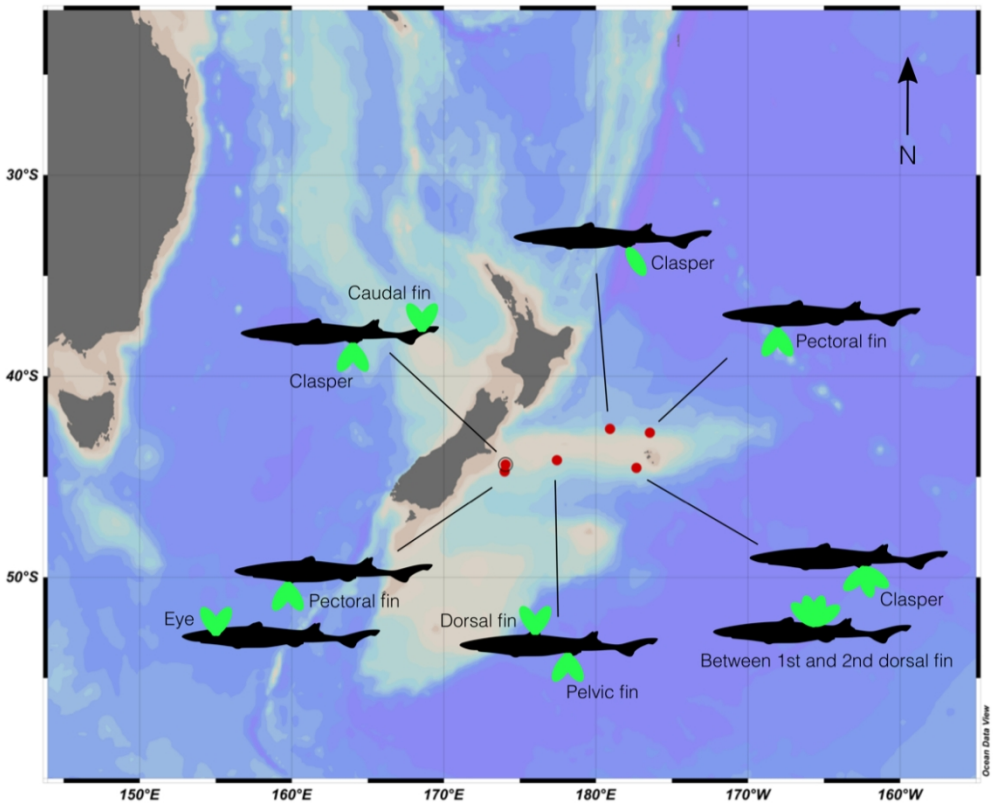

Figure 1. Map depicting the locations where *Etmopterus granulosus* infected with *Anelasma squalicola* were collected on Chatham Rise, New Zealand in January 2022. The number of parasitic barnacles and their site of infection on each host shark is indicated by the green ovals.

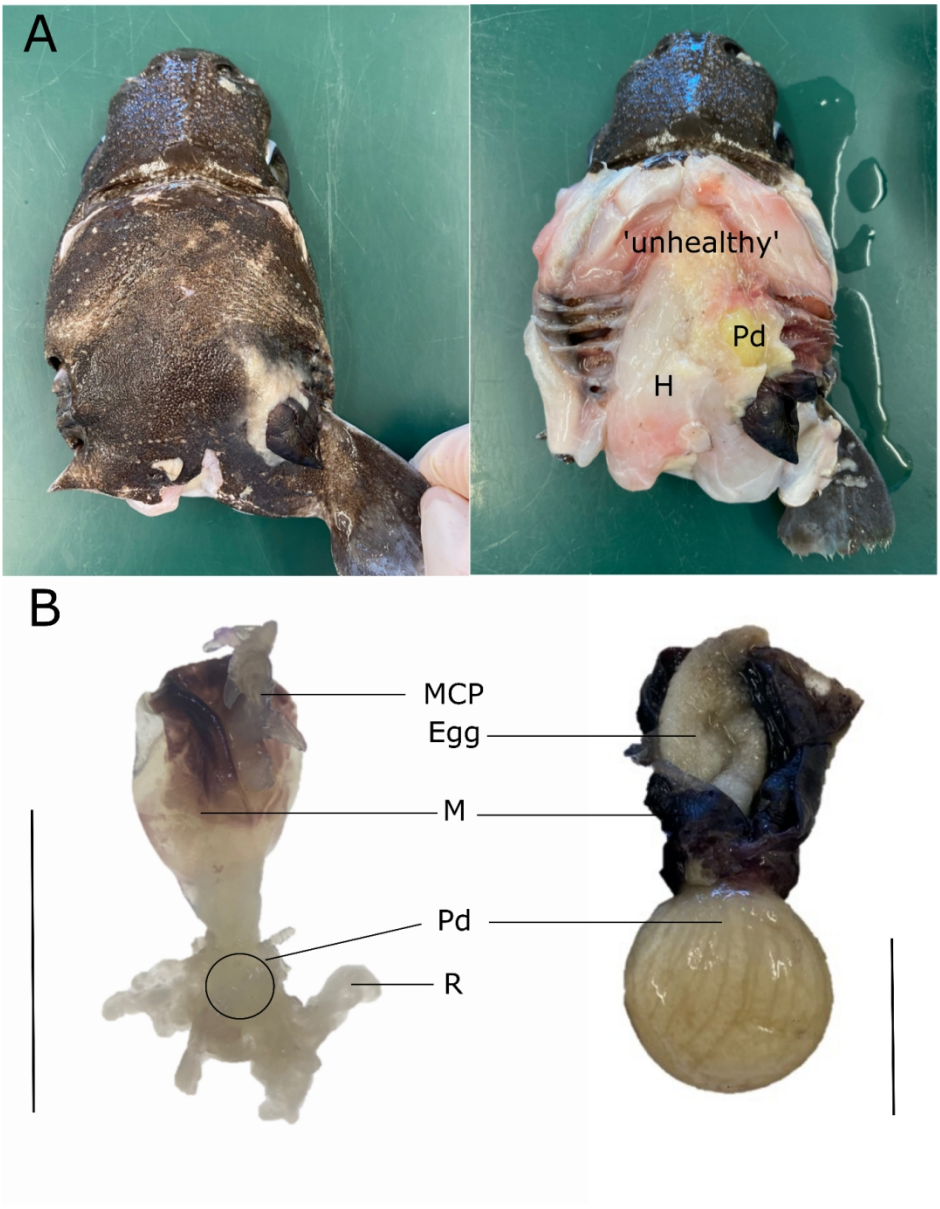

Figure 2. *Anelasma squalicola in situ* on *Etmopterus granulosus*. A) Pre-dissection photo of *A. squalicola* infecting *E. granulosus* (left) and partially dissected *A. squalicola* showing 'unhealthy' host tissue infested with *A. squalicola* rootlets, Pd, and healthy host tissue (H) (right). B) Two parasitic barnacles (varying in size) illustrating tissues taken for stable isotope analyses. These include mouth, cirri and penis (MCP), eggs (Egg), mantle (M), peduncle (Pd), and rootlets (R). Not represented is the inner mantle, a soft tissue found within the mantle. Scale bars represent 1 cm.

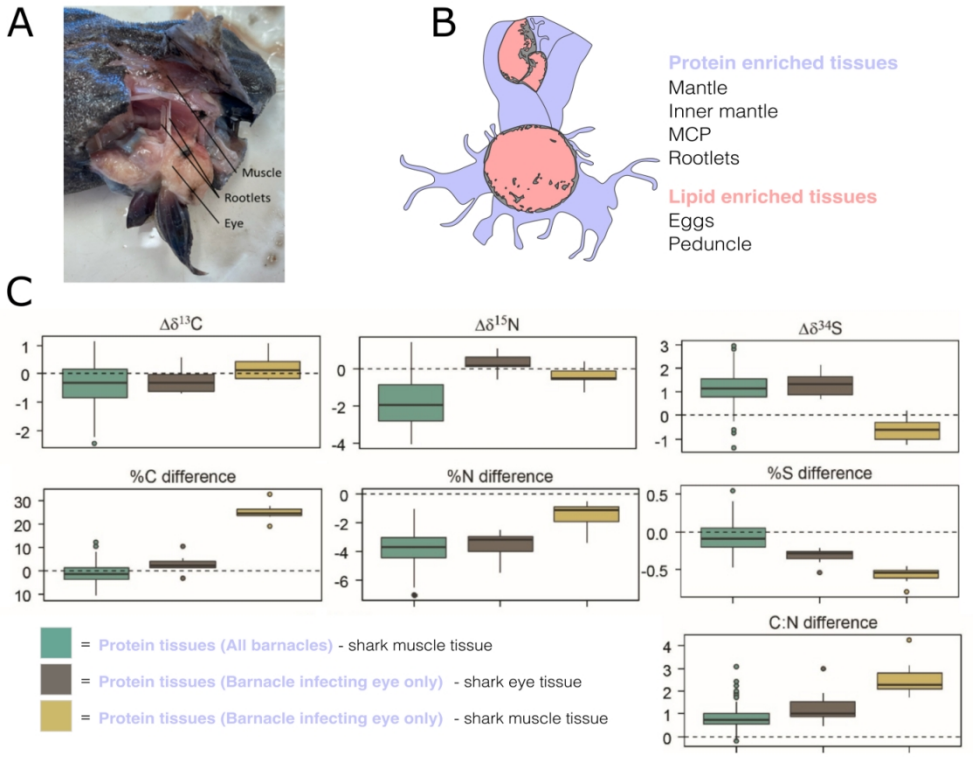

Figure 3. A) *A. squalicola in situ* of the right eye of *E. granulosus* whereby rootlets appear to have penetrated host cartilage for access to host muscle in the centre of the shark head. B) Visual characterisation of *A. squalicola* identified as either protein-rich (purple) or lipid- rich (pink) tissues. C) Stable isotope values and elemental compositions differences between parasite and host tissues. The difference between all barnacle 'protein tissues' (mean of all barnacles except individuals on shark no. 11 and their matching shark 'healthy' muscle tissues; green); the difference between shark no. 11's barnacle 'protein tissues' and the eye tissue of the shark (grey); and the difference between shark no. 11 barnacle's 'protein tissues' and the 'healthy' shark muscle tissue (yellow).

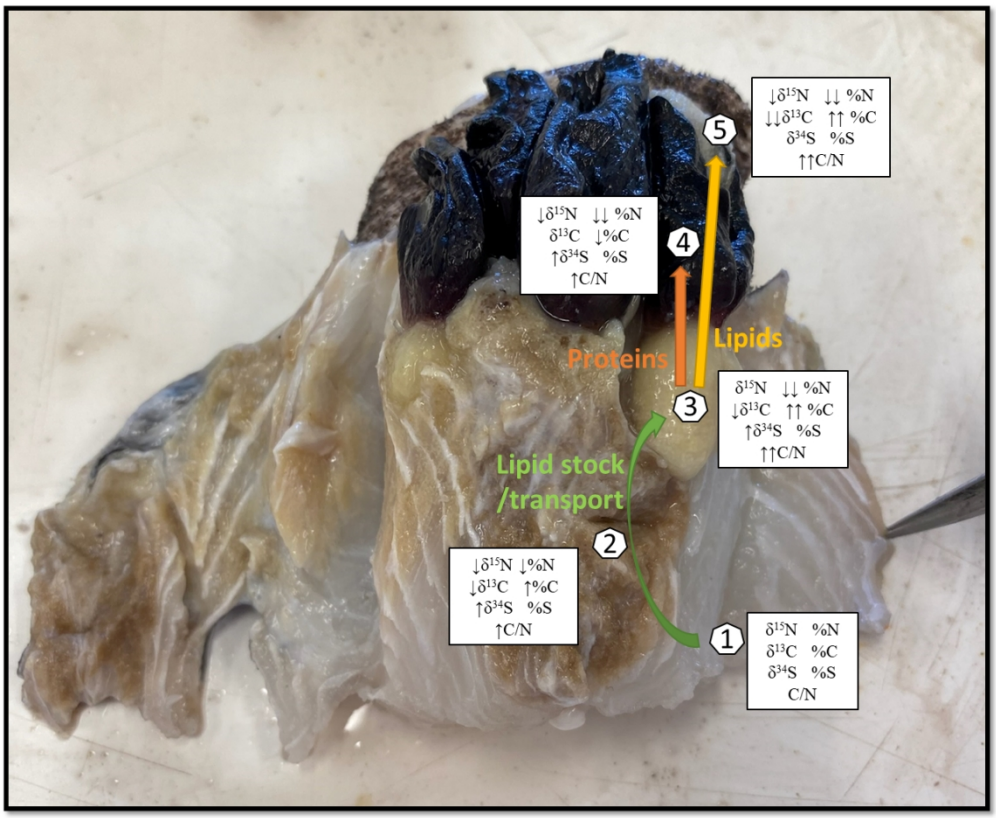

Figure 4. Proposed physiological mechanisms behind *A. squalicola*'s feeding strategy. (1) 'Healthy' shark muscle tissue, (2) 'unhealthy' shark tissue, (3) one of the barnacle's peduncle, (4) the same barnacle's protein tissues and (5) its egg stock. Green arrow represents a transfer of lipids and proteins via the barnacle's rootlets; Orange arrow represents a transfer of proteins for maintenance and yellow arrow represents a transfer of lipids to the next generation.

Tables

Unravelling the trophic interaction between a parasitic barnacle (*Anelasma squalicola*) and its host Southern lanternshark (*Etmopterus granulosus*) using stable isotopes

A.J.M. Sabadel[a,*], P. Cresson[b], B. Finucci[c] and J. Bennett[a]

[a]Department of Zoology, University of Otago, PO Box 56, Dunedin 9045, New Zealand

[b]IFREMER, Channel and North Sea Fisheries Research Unit, 150 Quai Gambetta, BP 699, 62 321 Boulogne sur Mer, France.

[c]National Institute of Water and Atmospheric Research (NIWA), 301 Evans Bay Parade, Hataitai 6021, Wellington, New Zealand

*Corresponding author: amandine.sabadel@otago.ac.nz

Table 1. Average stable isotope values of N, C and S, along with elemental compositions and C/N ratios of host shark *Etmopterus granulosus* and their parasitic barnacles *Anelasma squalicola*, collected from the Chatham Rise, New Zealand. Parasite tissues in *italic* are all part of the 'protein tissues' category. Note that SDs are not provided for the eye tissue as the measurement was made on one individual only.

Host Shark		**$\delta^{15}N$ (‰)**	**%N**	**$\delta^{13}C$ (‰)**	**%C**	**$\delta^{34}S$ (‰)**	**%S**	**C/N**
'Healthy' muscle (n = 10)	Avg.	12.0	15.5	-18.7	42.7	20.4	1.0	2.7
	SD	1.3	1.6	0.8	8.3	0.8	0.2	0.4
Eye (n = 1)	Avg.	8.9	14.6	-19.2	45.0	20.1	1.1	3.1
'Unhealthy' muscle (n = 4)	Avg.	11.5	13.5	-19.1	48.7	20.9	0.9	3.6
	SD	0.9	1.1	0.5	2.8	0.4	0.4	0.5
Parasitic barnacle								
Peduncle (n = 18)	Avg.	11.7	10.2	-19.9	56.3	21.0	0.7	6.6
	SD	1.6	3.3	1.7	11.1	1.0	0.3	3.5
Mantle (n = 18)	*Avg.*	*10.8*	*12.1*	*-19.1*	*48.7*	*21.5*	*0.9*	*4.1*
	SD	*2.7*	*1.8*	*0.8*	*6.4*	*0.8*	*0.5*	*0.9*
Inner mantle (n = 18)	*Avg.*	*10.1*	*12.1*	*-19.2*	*46.1*	*21.1*	*0.7*	*3.9*
	SD	*1.6*	*1.2*	*0.7*	*3.4*	*0.6*	*0.1*	*0.6*
Rootlets (n = 18)	*Avg.*	*10.8*	*12.9*	*-19.1*	*46.2*	*21.1*	*0.8*	*3.6*
	SD	*1.3*	*1.3*	*1.0*	*4.3*	*0.6*	*0.2*	*0.6*
Eggs (n = 11)	Avg.	11.0	6.2	-22.1	66.9	19.8	0.4	10.9
	SD	1.0	0.5	0.5	2.8	0.8	0.1	1.1
MCP (n = 19)	*Avg.*	*10.5*	*12.4*	*-18.8*	*44.0*	*21.6*	*0.9*	*3.6*
	SD	*1.4*	*0.8*	*0.5*	*2.4*	*0.5*	*0.1*	*0.4*
Protein tissues	***Avg.***	***10.6***	***12.3***	***-19.0***	***46.2***	***21.3***	***0.8***	***3.8***
	SD	***1.4***	***1.1***	***0.6***	***2.7***	***0.5***	***0.2***	***0.5***

Supplement

Unravelling the trophic interaction between a parasitic barnacle (*Anelasma squalicola*) and its host the Southern lanternshark (*Etmopterus granulosus*) using stable isotopes

A.J.M. Sabadel[a,*], P. Cresson[b] B. Finucci[c] and J. Bennett[a]

[a]Department of Zoology, University of Otago, PO Box 56, Dunedin 9045, New Zealand

[b]IFREMER, Channel and North Sea Fisheries Research Unit, 150 Quai Gambetta, BP 699, 62 321 Boulogne sur Mer, France.

[c]NIWA, 301 Evans Bay Parade, Hataitai 6021, Wellington, New Zealand

*Corresponding author: amandine.sabadel@otago.ac.nz

Figures

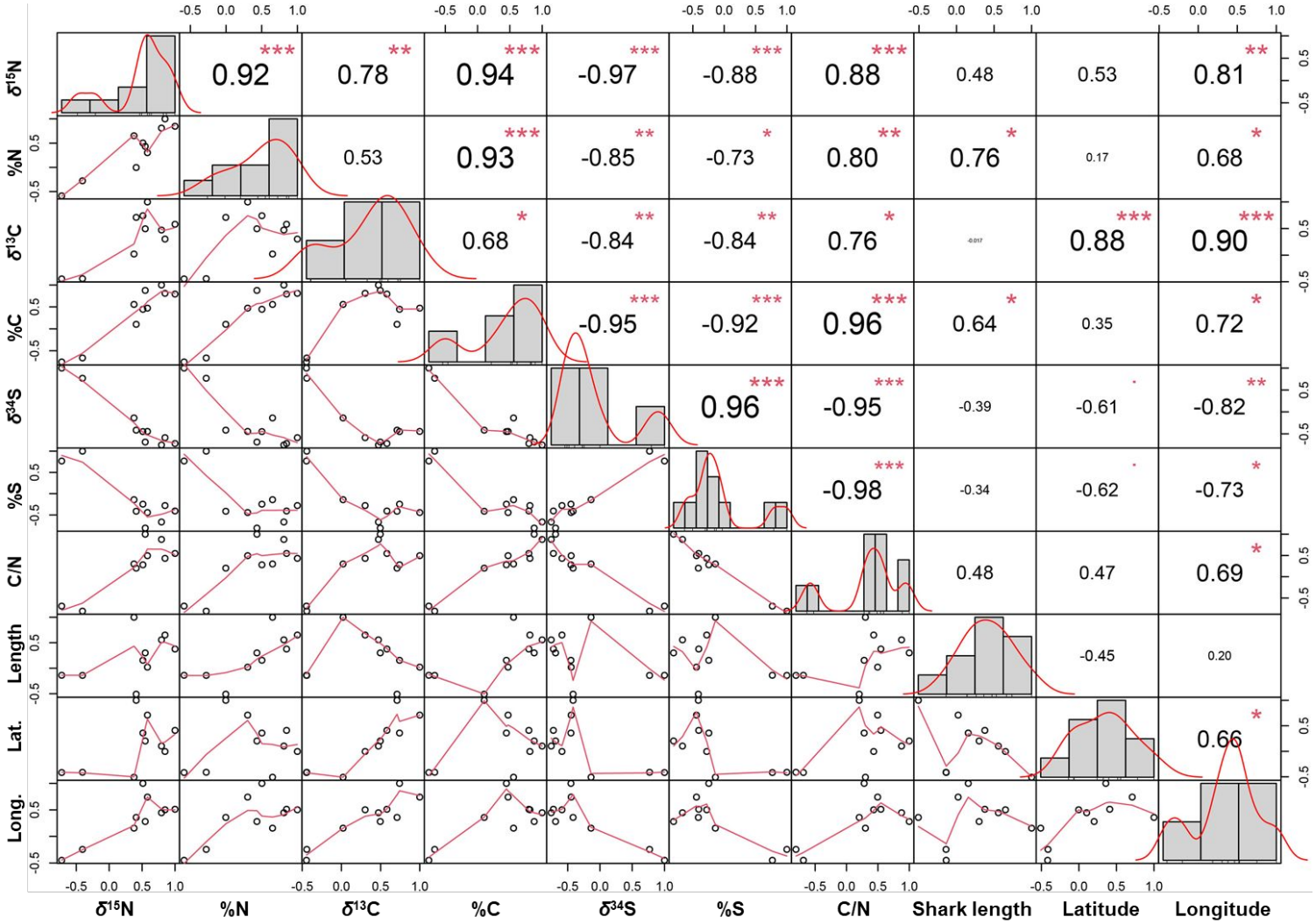

Figure S1. Correlation table of *E. granulosus*' muscle tissues stable isotope values, elemental compositions and C/N ratios. Values were also compared with shark length (Length) and shark location: latitude (Lat.) and longitude (Long.). Coefficients in upper triangle corresponds to R values and red stars represents the level of significance: no star = not significant, * = p value < 0.05, ** = 0.05 <p value < 0.001 and *** = p values << 0.001.

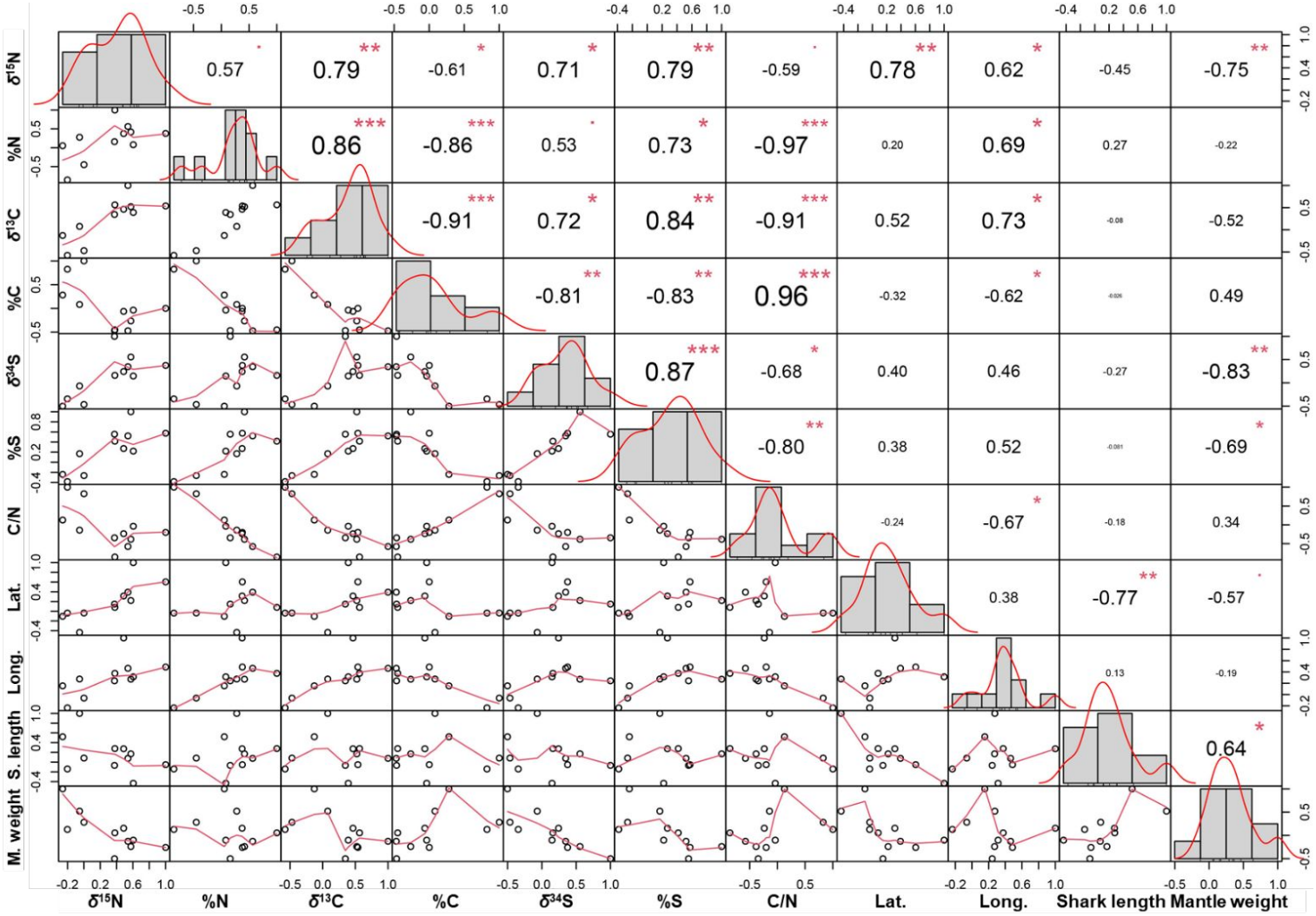

Figure S2. Correlation table of *A. squalicola*'s 'protein tissues' stable isotope values, elemental compositions and C/N ratios. Values were also compared with shark length (Length) and shark location: latitude (Lat.) and longitude (Long.) and barnacle weights (Mantle weight). Coefficients in upper triangle corresponds to R values and red stars represents the level of significance: no star = not significant, * = p value < 0.05, ** = 0.05 <p value < 0.001 and *** = p values << 0.001.

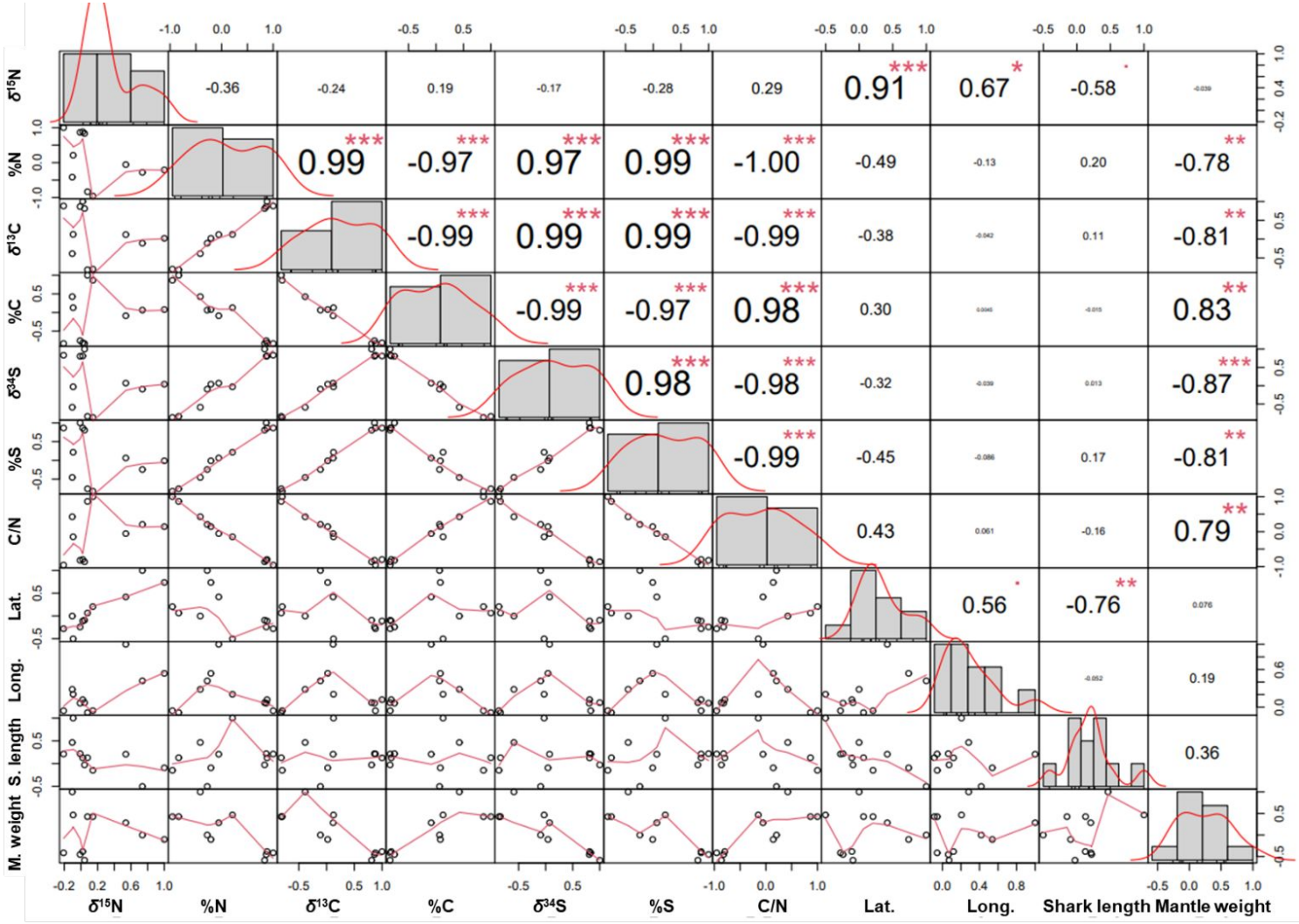

Figure S3. Correlation table of *A. squalicola*'s peduncle tissues stable isotope values, elemental compositions and C/N ratios. Values were also compared with shark length (Length) and shark location: latitude (Lat.) and longitude (Long.) and barnacle weights (Mantle weight). Coefficients in upper triangle corresponds to R values and red stars represents the level of significance: no star = not significant, * = p value < 0.05, ** = 0.05 <p value < 0.001 and *** = p values << 0.001.

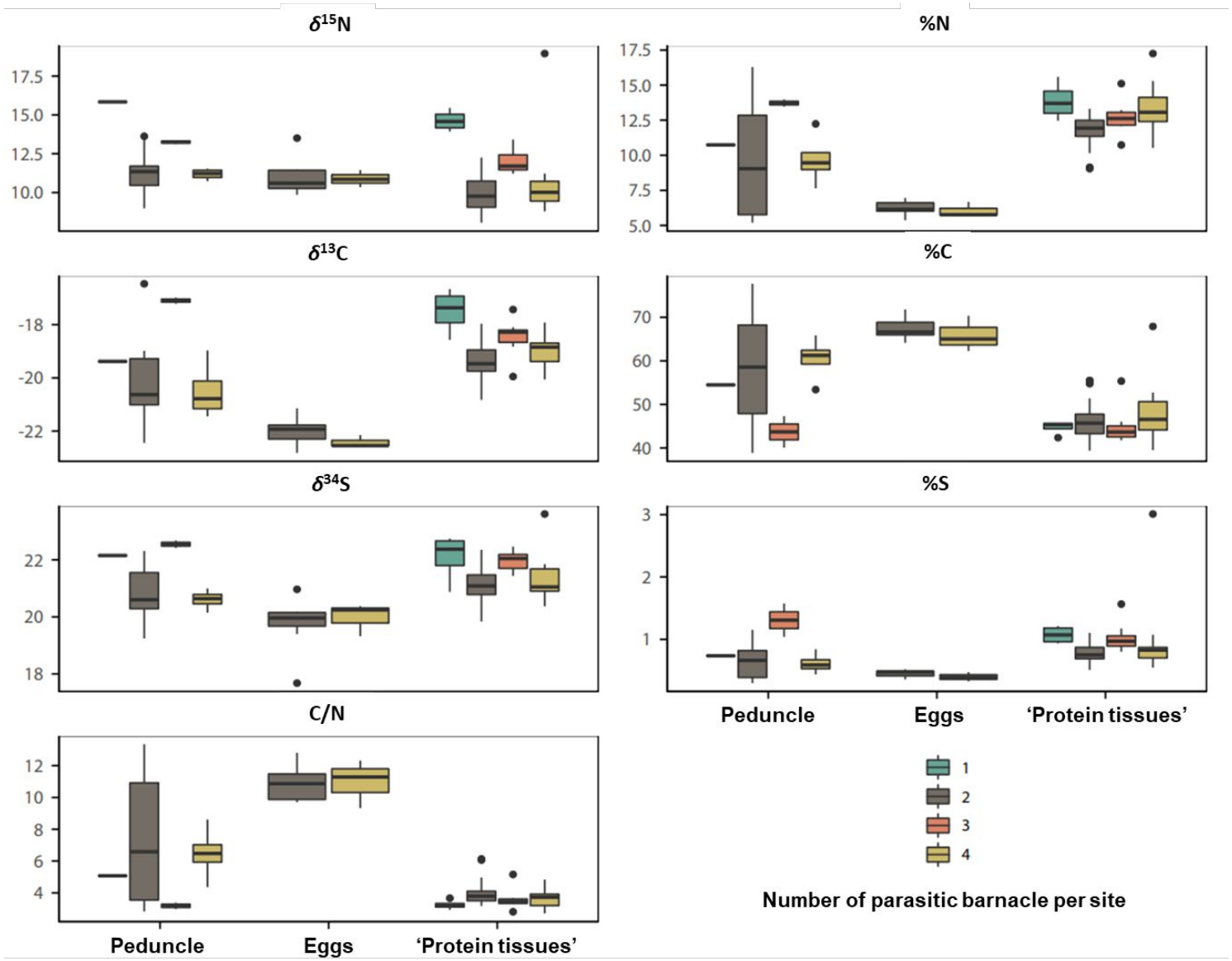

Figure S4. Boxplot highlighting the relationship between the number of *A. squalicola* per infection site on stable isotope values (δ^{15}N, δ^{13}C and δ^{34}S), elemental compositions (%N, %C and %S) and the C/N ratio.

Tables

Table S1. Difference between host shark or parasitic barnacle tissues vs host shark 'healthy' muscle tissues for the different stable isotope values, elemental composition, and C/N ratio.

Host Shark		**$\delta^{15}N$ (‰)**	**%N**	**$\delta^{13}C$ (‰)**	**%C**	**$\delta^{34}S$ (‰)**	**%S**	**C/N**
Δ'unhealthy'-'healthy' muscle	Avg.	-1.0	-3.3	-0.7	0.7	0.7	-0.1	0.8
	SD	0.9	1.5	0.4	1.6	0.6	0.2	0.4
ΔEye-'healthy' muscle	Avg.	-0.7	2.1	0.5	n/a	-1.9	-0.3	n/a
	SD	n/a	n/a	n/a	n/a	n/a	n/a	n/a
Parasitic barnacle								
ΔPeduncle-'healthy' muscle	Avg.	-0.4	-5.6	-1.1	9.2	1.0	-0.1	3.2
	SD	1.4	3.0	1.8	11.2	1.0	0.3	3.1
ΔEggs-'healthy' muscle	Avg.	-1.2	-9.6	-3.6	19.5	0.0	-0.4	7.7
	SD	1.1	1.5	0.5	4.4	0.4	0.1	1.1
ΔProtein tissues-'healthy' muscle	Avg.	-1.8	-3.7	-0.4	-0.9	1.2	-0.1	0.8
	SD	1.3	1.1	0.7	4.4	0.7	0.2	0.5

Table S2. ANOVA tests isotopic ratios. Results for eyes should be taken with caution, as based on only one value.

Variable	Statistic	p value		Post hoc
$\delta^{15}N$	$F_{109,8} = 2.14$	0.04	*	$Eye^{ab} = Inner\ mantle^{a} = MCP^{ab} = Rootlets^{ab} = Mantle^{ab} = Eggs^{ab} =$ 'Unhealthy' shark $muscle^{ab} = Peduncle^{ab} =$ 'Healthy' shark $muscle^{b}$
%N	$F_{109,8} = 24.64$	$<2.2\ 10^{-16}$	***	$Eggs^{a} < Peduncle^{b} < Mantle^{c} = Inner\ mantle^{c} = MCP^{cd} = Rootlets^{c} =$ 'Unhealthy' shark $muscle^{cd} = Eye^{abc} <$ 'Healthy' shark $muscle^{d}$
$\delta^{13}C$	$F_{108,8} = 14.16$	$6.3\ 10^{-14}$	***	$Eggs^{a} < Peduncle^{b} =$ 'Unhealthy' shark $muscle^{bc} = Inner\ mantle^{bc} = Eye^{bc} = Rootlets^{bc} = Mantle^{bc} < MCP^{c} =$ 'Healthy' shark $muscle^{c}$
%C	$F_{109,8} = 18.48$	$<2.2\ 10^{-16}$	***	$MCP^{a} =$ 'Healthy' shark $muscle^{a} = Eye^{a} = Inner\ mantle^{a} = Rootlets^{a} = Mantle^{a} =$ 'Unhealthy' shark $muscle^{a} < Peduncle^{b} < Eggs^{c}$
$\delta^{34}S$	$F_{109,8} = 7.78$	$3.2\ 10^{-8}$	***	$Eggs^{a} \leq Eye^{ab} =$ 'Healthy' shark $muscle^{ab} =$ 'Unhealthy' shark $muscle^{ab} < Peduncle^{bc} = Rootlets^{bc} = Inner\ mantle^{bc} = Mantle^{bc} = MCP^{bc}$
%S	$F_{109,8} = 3.98$	$3.6\ 10^{-4}$	***	$Eggs^{a} \leq Peduncle^{ab} = Inner\ mantle^{ab} \leq Rootlets^{b} = MCP^{b} \leq$ 'Unhealthy' shark $muscle^{ab} < Mantle^{b} =$ 'Healthy' shark $muscle^{b} = Eye^{ab}$
C:N	$F_{109,8} = 32.43$	$<2.2\ 10^{-16}$	***	'Healthy' shark $muscle^{a} = Eye^{a} = MCP^{a} = Rootlets^{a} =$ 'Unhealthy' shark $muscle^{a} = Inner\ mantle^{a} = Mantle^{a} < Peduncle^{b} < Eggs^{c}$

Shark no.	Sample ID	$\delta^{15}N$ (‰)	%N	$\delta^{13}C$ (‰)	%C	$\delta^{34}S$ (‰)	%S	C/N	Station
3	S3S1B1B2_SKN	n/a	n/a	n/a	n/a	n/a	n/a	n/a	86
3	S3S2B1B2_SKN	12.3	15.9	-19.3	45.2	19.6	1.0	2.8	86
4	S4S1B1B2_SKN	11.9	14.5	-19.0	44.1	20.1	0.8	3.0	99
4	S4S2B1B2_SKN	12.1	15.6	-18.6	48.6	20.2	0.8	3.1	99
8	S8S2B1B2_SKN	11.5	14.0	-17.6	43.1	20.0	0.7	3.1	40
10	S10S2B1_SKN	14.0	17.0	-17.8	45.1	19.8	1.0	2.6	95
11	S11S2B1B2_SKN	9.6	12.6	-19.6	22.9	22.0	1.3	1.8	100
12	S12S2B1B2_SKN	11.5	16.1	-19.5	43.3	21.2	1.0	2.7	100
16	S16S2B1B2B3B4_SKN	12.5	17.0	-18.6	49.7	19.8	0.8	2.9	66
16	S16S2B1B2B3B4_SKN_2	12.6	17.6	-18.5	50.0	19.6	0.9	2.8	66
17	S17S2B1B2B3B4_SKN	12.5	16.2	-18.1	47.1	21.0	1.2	2.9	66
17	S17S2B1B2B3_SKN_2	12.4	16.6	-18.6	45.0	20.4	1.0	2.7	66

Latitude	Longiture	Avg. depth	Shark sex	Shark maturity	Shark length (cm)
-44.2	177.4	929	male	3	39.6
-44.2	177.4	929	male	3	39.6
-44.4	174.1	707	male	3	61
-44.4	174.1	707	male	3	61
-42.8	183.5	1026	male	3	38.1
-42.6	180.9	1261	male	1	52.6
-44.7	174.0	841	male	1 or 2	43
-44.7	174.0	841	female	2	63
-44.6	182.7	813	female	6	71.1
-44.6	182.7	813	female	6	71.1
-44.6	182.7	813	male	3	62.7
-44.6	182.7	813	male	3	62.7

Shark weight (g)	no. of infected sites	Site 1 - location	Site 1 - no. of barnacles
200	2	dorsal fin	2
200	2	dorsal fin	2
1130	2	tail	2
1130	2	tail	2
150	1	along the arm fin	2
785	1	clasper	1
355	1	eye	2
1410	1	pectoral fin	2
1950	1	on the back	4
1950	1	on the back	4
1145	1	clasper	3
1145	1	clasper	3

Site 2 - location	Site 2 - no. of barnacles
pelvic fin	2
pelvic fin	2
clapser	2
clapser	2
n/a	n/a
n/a	n/a
n/a	n/a
n/a	n/a
n/a	n/a
n/a	n/a
n/a	n/a
n/a	n/a

Shark no.	Sample ID	Mantle weight (mg)	Estimated barnacle size	$\delta^{15}N$ (‰)	%N
3	S3S1B1_BUL	61.97	Medium	n/a	n/a
3	S3S1B2_BUL	20.81	Small	10.0	13.1
3	S3S2B1_BUL	14.39	Small	11.0	11.2
3	S3S2B2_BUL	5.63	Small	11.3	12.8
4	S4S1B1_BUL	94.59	Medium	n/a	n/a
4	S4S1B2_BUL	100.58	Large	11.7	12.9
4	S4S2B1_BUL	113.44	Large	n/a	n/a
4	S4S2B2_BUL	62.46	Medium	11.7	8.4
8	S8S2B1_BUL	87.59	Medium	13.6	5.5
8	S8S2B2_BUL	223.44	Large	13.5	5.8
10	S10S2B1_BUL	30.35	Small	15.8	10.7
11	S11S2B1_BUL	66.62	Medium	10.6	5.7
11	S11S2B2_BUL	15.63	Small	10.3	9.0
12	S12S2B1_BUL	188.90	Large	11.5	5.2
12	S12S2B2_BUL	118.56	Large	9.0	16.3
16	S16S2B1_BUL	138.84	Large	11.5	7.6
16	S16S2B2_BUL	226.67	Large	10.7	9.5
16	S16S2B3_BUL	182.37	Large	11.4	9.4
16	S16S2B4_BUL	159.34	Large	11.0	12.2
17	S17S2B1_BUL	16.33	Small	13.1	13.5
17	S17S2B2_BUL	16.98	Small	13.4	14.0
17	S17S2B3_BUL	4.85	Small	n/a	n/a

$\delta^{13}C$ (‰)	%C	$\delta^{34}S$ (‰)	%S	C/N	Station	Latitude	Longiture	Avg. depth	Shark sex
n/a	n/a	n/a	n/a	n/a	86	-44.2	177.4	929	male
-19.4	38.9	22.3	0.8	3.0	86	-44.2	177.4	929	male
-20.6	52.3	21.4	0.8	4.7	86	-44.2	177.4	929	male
-19.0	41.4	21.7	0.8	3.2	86	-44.2	177.4	929	male
n/a	n/a	n/a	n/a	n/a	99	-44.4	174.1	707	male
-19.2	49.8	20.6	0.8	3.9	99	-44.4	174.1	707	male
n/a	n/a	n/a	n/a	n/a	99	-44.4	174.1	707	male
-21.8	77.7	20.2	0.7	9.3	99	-44.4	174.1	707	male
-20.9	69.2	19.2	0.4	12.5	40	-42.8	183.5	1026	male
-20.8	58.6	20.3	0.4	10.0	40	-42.8	183.5	1026	male
-19.4	54.5	22.2	0.7	5.1	95	-42.6	180.9	1261	male
-21.1	67.2	20.5	0.4	11.8	100	-44.7	174.0	841	male
-20.6	59.5	21.0	0.6	6.6	100	-44.7	174.0	841	male
-22.4	69.3	19.4	0.3	13.3	100	-44.7	174.0	841	female
-16.5	46.0	21.9	1.2	2.8	100	-44.7	174.0	841	female
-21.4	65.8	20.1	0.4	8.6	66	-44.6	182.7	813	female
-21.1	61.3	20.7	0.6	6.4	66	-44.6	182.7	813	female
-20.5	61.2	20.6	0.6	6.5	66	-44.6	182.7	813	female
-19.0	53.4	21.0	0.8	4.4	66	-44.6	182.7	813	female
-17.2	40.1	22.4	1.6	3.0	66	-44.6	182.7	813	male
-17.0	47.3	22.7	1.0	3.4	66	-44.6	182.7	813	male
n/a	n/a	n/a	n/a	n/a	66	-44.6	182.7	813	male

Shark maturity	Shark length (cm)	Shark weight (g)	no. of infected sites
3	39.6	200	2
3	39.6	200	2
3	39.6	200	2
3	39.6	200	2
3	61	1130	2
3	61	1130	2
3	61	1130	2
3	61	1130	2
3	38.1	150	1
3	38.1	150	1
1	52.6	785	1
1 or 2	43	355	1
2 or 2	43	355	1
2	63	1410	1
2	63	1410	1
6	71.1	1950	1
6	71.1	1950	1
6	71.1	1950	1
6	71.1	1950	1
3	62.7	1145	1
3	62.7	1145	1
3	62.7	1145	1

Site 1 - location	Site 1 - no. of barnacles	Site 2 - location	Site 2 - no. of barnacles
dorsal fin	2	pelvic fin	2
dorsal fin	2	pelvic fin	2
dorsal fin	2	pelvic fin	2
dorsal fin	2	pelvic fin	2
tail	2	clapser	2
tail	2	clapser	2
tail	2	clapser	2
tail	2	clapser	2
along the arm fin	2	n/a	n/a
along the arm fin	2	n/a	n/a
clasper	1	n/a	n/a
eye	2	n/a	n/a
eye	2	n/a	n/a
pectoral fin	2	n/a	n/a
pectoral fin	2	n/a	n/a
on the back	4	n/a	n/a
on the back	4	n/a	n/a
on the back	4	n/a	n/a
on the back	4	n/a	n/a
clasper	3	n/a	n/a
clasper	3	n/a	n/a
clasper	3	n/a	n/a

Shark no.	Sample ID	Mantle weight (mg)	Estimated barnacle size	$\delta^{15}N$ (‰)	%N
3	S3S1B1_OSH	61.97	Medium	n/a	n/a
3	S3S1B2_OSH	20.81	Small	n/a	n/a
3	S3S2B1_OSH	14.39	Small	n/a	n/a
3	S3S2B2_OSH	5.63	Small	10.4	12.3
4	S4S1B1_OSH	94.59	Medium	10.0	11.8
4	S4S1B2_OSH	100.58	Large	8.8	11.0
4	S4S2B1_OSH	113.44	Large	n/a	n/a
4	S4S2B2_OSH	62.46	Medium	8.2	11.3
8	S8S2B1_OSH	87.59	Medium	10.8	11.5
8	S8S2B2_OSH	223.44	Large	12.3	9.0
10	S10S2B1_OSH	30.35	Small	15.4	14.2
11	S11S2B1_OSH	66.62	Medium	9.1	9.1
11	S11S2B2_OSH	15.63	Small	8.3	11.6
12	S12S2B1_OSH	188.90	Large	9.3	12.2
12	S12S2B2_OSH	118.56	Large	8.6	11.7
16	S16S2B1_OSH	138.84	Large	9.2	10.5
16	S16S2B2_OSH	226.67	Large	11.2	12.4
16	S16S2B3_OSH	182.37	Large	19.0	17.2
16	S16S2B4_OSH	159.34	Large	9.5	13.0
17	S17S2B1_OSH	16.33	Small	11.4	12.7
17	S17S2B2_OSH	16.98	Small	11.3	12.6
17	S17S2B3_OSH	4.85	Small	12.5	13.2

$\delta^{13}C$ (‰)	%C	$\delta^{34}S$ (‰)	%S	C/N	Station	Latitude	Longiture	Avg. depth	Shark sex
n/a	n/a	n/a	n/a	n/a	86	-44.2	177.4	929	male
n/a	n/a	n/a	n/a	n/a	86	-44.2	177.4	929	male
n/a	n/a	n/a	n/a	n/a	86	-44.2	177.4	929	male
-18.9	41.7	21.8	0.6	3.4	86	-44.2	177.4	929	male
-19.1	48.3	20.5	1.0	4.1	99	-44.4	174.1	707	male
-19.6	50.2	20.7	0.7	4.6	99	-44.4	174.1	707	male
n/a	n/a	n/a	n/a	n/a	99	-44.4	174.1	707	male
-19.6	42.6	21.7	0.9	3.8	99	-44.4	174.1	707	male
-18.3	47.3	20.8	0.8	4.1	40	-42.8	183.5	1026	male
-20.0	55.5	20.7	0.7	6.1	40	-42.8	183.5	1026	male
-17.0	45.1	22.7	1.2	3.2	95	-42.6	180.9	1261	male
-19.8	55.5	20.8	0.5	6.1	100	-44.7	174.0	841	male
-19.5	47.3	22.2	0.8	4.1	100	-44.7	174.0	841	male
-19.0	45.7	20.6	0.7	3.8	100	-44.7	174.0	841	female
-19.8	49.5	21.5	0.9	4.2	100	-44.7	174.0	841	female
-20.1	50.9	21.0	0.6	4.8	66	-44.6	182.7	813	female
-19.2	52.7	21.2	0.9	4.2	66	-44.6	182.7	813	female
n/a	67.9	23.6	3.0	3.9	66	-44.6	182.7	813	female
-19.6	41.6	21.8	0.8	3.2	66	-44.6	182.7	813	female
-18.1	46.1	21.6	0.9	3.6	66	-44.6	182.7	813	male
-18.4	45.3	21.9	0.9	3.6	66	-44.6	182.7	813	male
-18.3	43.9	22.1	1.0	3.3	66	-44.6	182.7	813	male

Shark maturity	Shark length (cm)	Shark weight (g)	no. of infected sites
3	39.6	200	2
3	39.6	200	2
3	39.6	200	2
3	39.6	200	2
3	61	1130	2
3	61	1130	2
3	61	1130	2
3	61	1130	2
3	38.1	150	1
3	38.1	150	1
1	52.6	785	1
1 or 2	43	355	1
2 or 2	43	355	1
2	63	1410	1
2	63	1410	1
6	71.1	1950	1
6	71.1	1950	1
6	71.1	1950	1
6	71.1	1950	1
3	62.7	1145	1
3	62.7	1145	1
3	62.7	1145	1

Site 1 - location	Site 1 - no. of barnacles	Site 2 - location	Site 2 - no. of barnacles
dorsal fin	2	pelvic fin	2
dorsal fin	2	pelvic fin	2
dorsal fin	2	pelvic fin	2
dorsal fin	2	pelvic fin	2
tail	2	clapser	2
tail	2	clapser	2
tail	2	clapser	2
tail	2	clapser	2
along the arm fin	2	n/a	n/a
along the arm fin	2	n/a	n/a
clasper	1	n/a	n/a
eye	2	n/a	n/a
eye	2	n/a	n/a
pectoral fin	2	n/a	n/a
pectoral fin	2	n/a	n/a
on the back	4	n/a	n/a
on the back	4	n/a	n/a
on the back	4	n/a	n/a
on the back	4	n/a	n/a
clasper	3	n/a	n/a
clasper	3	n/a	n/a
clasper	3	n/a	n/a

Shark no.	Sample ID	Mantle weight (mg)	Estimated barnacle size	$\delta^{15}N$ (‰)	%N	$\delta^{13}C$ (‰)
3	S3S1B1_ISH	61.97	Medium	8.4	12.9	-19.0
3	S3S1B2_ISH	20.81	Small	9.7	11.5	-19.5
3	S3S2B1_ISH	14.39	Small	10.3	12.4	-20.0
3	S3S2B2_ISH	5.63	Small	n/a	n/a	n/a
4	S4S1B1_ISH	94.59	Medium	8.1	11.2	-18.6
4	S4S1B2_ISH	100.58	Large	9.0	10.3	-19.9
4	S4S2B1_ISH	113.44	Large	n/a	n/a	n/a
4	S4S2B2_ISH	62.46	Medium	9.8	12.2	-19.4
8	S8S2B1_ISH	87.59	Medium	n/a	n/a	n/a
8	S8S2B2_ISH	223.44	Large	11.4	11.9	-18.5
10	S10S2B1_ISH	30.35	Small	14.2	12.5	-18.6
11	S11S2B1_ISH	66.62	Medium	9.7	10.2	-19.7
11	S11S2B2_ISH	15.63	Small	8.9	11.1	-19.5
12	S12S2B1_ISH	188.90	Large	10.9	13.2	-18.5
12	S12S2B2_ISH	118.56	Large	8.4	12.8	-20.5
16	S16S2B1_ISH	138.84	Large	10.1	11.7	-19.3
16	S16S2B2_ISH	226.67	Large	8.8	12.3	-19.5
16	S16S2B3_ISH	182.37	Large	9.0	13.2	-18.4
16	S16S2B4_ISH	159.34	Large	10.8	15.3	-17.9
17	S17S2B1_ISH	16.33	Small	12.9	10.7	-20.0
17	S17S2B2_ISH	16.98	Small	11.2	12.1	-18.8
17	S17S2B3_ISH	4.85	Small	n/a	n/a	n/a

%C	$\delta^{34}S$ (‰)	%S	C/N	Station	Latitude	Longiture	Avg. depth	Shark sex	Shark maturity
44.6	20.7	0.6	3.5	86	-44.2	177.4	929	male	3
43.0	21.1	0.5	3.7	86	-44.2	177.4	929	male	3
45.6	21.0	0.8	3.7	86	-44.2	177.4	929	male	3
n/a	n/a	n/a	n/a	86	-44.2	177.4	929	male	3
39.4	21.1	0.8	3.5	99	-44.4	174.1	707	male	3
46.9	20.9	0.7	4.5	99	-44.4	174.1	707	male	3
n/a	n/a	n/a	n/a	99	-44.4	174.1	707	male	3
46.5	21.2	0.9	3.8	99	-44.4	174.1	707	male	3
n/a	n/a	n/a	n/a	40	-42.8	183.5	1026	male	3
45.2	21.1	0.7	3.8	40	-42.8	183.5	1026	male	3
45.7	22.1	1.0	3.7	95	-42.6	180.9	1261	male	1
50.4	21.4	0.8	5.0	100	-44.7	174.0	841	male	1 or 2
47.7	21.5	0.7	4.3	100	-44.7	174.0	841	male	2 or 2
44.8	19.8	0.7	3.4	100	-44.7	174.0	841	female	2
44.0	21.9	0.7	3.4	100	-44.7	174.0	841	female	2
50.5	20.5	0.7	4.3	66	-44.6	182.7	813	female	6
46.1	21.1	0.5	3.7	66	-44.6	182.7	813	female	6
44.8	20.4	0.7	3.4	66	-44.6	182.7	813	female	6
44.9	21.0	0.8	2.9	66	-44.6	182.7	813	female	6
55.3	21.4	0.8	5.2	66	-44.6	182.7	813	male	3
44.3	22.1	0.9	3.7	66	-44.6	182.7	813	male	3
n/a	n/a	n/a	n/a	66	-44.6	182.7	813	male	3

Shark length (cm)	Shark weight (g)	no. of infected sites	Site 1 - location
39.6	200	2	dorsal fin
39.6	200	2	dorsal fin
39.6	200	2	dorsal fin
39.6	200	2	dorsal fin
61	1130	2	tail
61	1130	2	tail
61	1130	2	tail
61	1130	2	tail
38.1	150	1	along the arm fin
38.1	150	1	along the arm fin
52.6	785	1	clasper
43	355	1	eye
43	355	1	eye
63	1410	1	pectoral fin
63	1410	1	pectoral fin
71.1	1950	1	on the back
71.1	1950	1	on the back
71.1	1950	1	on the back
71.1	1950	1	on the back
62.7	1145	1	clasper
62.7	1145	1	clasper
62.7	1145	1	clasper

Site 1 - no. of barnacles	Site 2 - location	Site 2 - no. of barnacles
2	pelvic fin	2
2	pelvic fin	2
2	pelvic fin	2
2	pelvic fin	2
2	clapser	2
2	clapser	2
2	clapser	2
2	clapser	2
2	n/a	n/a
2	n/a	n/a
1	n/a	n/a
2	n/a	n/a
2	n/a	n/a
2	n/a	n/a
2	n/a	n/a
4	n/a	n/a
4	n/a	n/a
4	n/a	n/a
4	n/a	n/a
3	n/a	n/a
3	n/a	n/a
3	n/a	n/a

Shark no.	Sample ID	Mantle weight (mg)	Estimated barnacle size	$\delta^{15}N$ (‰)	%N
3	S3S1B1_TEN	61.97	Medium	9.5	13.2
3	S3S1B2_TEN	20.81	Small	10.0	11.4
3	S3S2B1_TEN	14.39	Small	11.1	12.3
3	S3S2B2_TEN	5.63	Small	10.3	12.5
4	S4S1B1_TEN	94.59	Medium	9.2	10.6
4	S4S1B2_TEN	100.58	Large	10.9	11.3
4	S4S2B1_TEN	113.44	Large	10.7	12.2
4	S4S2B2_TEN	62.46	Medium	n/a	n/a
8	S8S2B1_TEN	87.59	Medium	n/a	n/a
8	S8S2B2_TEN	223.44	Large	n/a	n/a
10	S10S2B1_TEN	30.35	Small	13.9	15.6
11	S11S2B1_TEN	66.62	Medium	n/a	n/a
11	S11S2B2_TEN	15.63	Small	10.0	12.1
12	S12S2B1_TEN	188.90	Large	10.9	13.3
12	S12S2B2_TEN	118.56	Large	10.2	12.8
16	S16S2B1_TEN	138.84	Large	11.0	13.4
16	S16S2B2_TEN	226.67	Large	10.7	14.0
16	S16S2B3_TEN	182.37	Large	9.0	13.2
16	S16S2B4_TEN	159.34	Large	10.0	15.0
17	S17S2B1_TEN	16.33	Small	13.4	15.1
17	S17S2B2_TEN	16.98	Small	11.7	12.3
17	S17S2B3_TEN	4.85	Small	11.7	12.6

$\delta^{13}C$ (‰)	%C	$\delta^{34}S$ (‰)	%S	C/N	%S	C/N	Longiture	Avg. depth	Shark sex
-19.0	42.7	20.7	0.7	3.2	86	-44.17133	177.43567	929	male
-19.4	41.7	21.2	0.5	3.7	86	-44.17133	177.43567	929	male
-20.3	50.5	20.4	0.7	4.1	86	-44.17133	177.43567	929	male
-19.7	42.0	21.6	0.6	3.4	86	-44.17133	177.43567	929	male
-19.4	48.6	20.9	0.7	4.6	99	-44.3915	174.057	707	male
-20.8	54.8	20.4	0.7	4.8	99	-44.3915	174.057	707	male
-19.8	46.7	21.1	0.9	3.8	99	-44.3915	174.057	707	male
n/a	n/a	n/a	n/a	n/a	99	-44.3915	174.057	707	male
n/a	n/a	n/a	n/a	n/a	40	-42.805	183.5485	1026	male
n/a	n/a	n/a	n/a	n/a	40	-42.805	183.5485	1026	male
-16.7	45.6	20.9	0.9	2.9	95	-42.61633	180.926	1261	male
n/a	n/a	n/a	n/a	n/a	100	-44.73317	174.00167	841	male
-19.8	46.2	21.0	0.8	3.8	100	-44.73317	174.00167	841	male
-19.1	47.8	20.5	0.7	3.6	100	-44.73317	174.00167	841	female
-19.8	51.4	21.1	0.7	4.0	100	-44.73317	174.00167	841	female
-18.7	49.7	20.9	0.7	3.7	66	-44.55583	182.66417	813	female
-19.8	52.4	20.4	0.7	3.8	66	-44.55583	182.66417	813	female
-18.3	42.1	21.0	0.6	3.2	66	-44.55583	182.66417	813	female
-19.0	41.6	20.9	0.9	2.8	66	-44.55583	182.66417	813	female
-17.4	42.4	22.2	1.6	2.8	66	-44.55583	182.66417	813	male
-18.7	41.8	22.4	1.2	3.4	66	-44.55583	182.66417	813	male
-18.2	42.9	21.5	1.0	3.4	66	-44.55583	182.66417	813	male

Shark maturity	Shark length (cm)	Shark weight (g)	no. of infected sites
3	39.6	200	2
3	39.6	200	2
3	39.6	200	2
3	39.6	200	2
3	61	1130	2
3	61	1130	2
3	61	1130	2
3	61	1130	2
3	38.1	150	1
3	38.1	150	1
1	52.6	785	1
1 or 2	43	355	1
2 or 2	43	355	1
2	63	1410	1
2	63	1410	1
6	71.1	1950	1
6	71.1	1950	1
6	71.1	1950	1
6	71.1	1950	1
3	62.7	1145	1
3	62.7	1145	1
3	62.7	1145	1

Site 1 - location	Site 1 - no. of barnacles	Site 2 - location	Site 2 - no. of barnacles
dorsal fin	2	pelvic fin	2
dorsal fin	2	pelvic fin	2
dorsal fin	2	pelvic fin	2
dorsal fin	2	pelvic fin	2
tail	2	clapser	2
tail	2	clapser	2
tail	2	clapser	2
tail	2	clapser	2
along the arm fin	2	n/a	n/a
along the arm fin	2	n/a	n/a
clasper	1	n/a	n/a
eye	2	n/a	n/a
eye	2	n/a	n/a
pectoral fin	2	n/a	n/a
pectoral fin	2	n/a	n/a
on the back	4	n/a	n/a
on the back	4	n/a	n/a
on the back	4	n/a	n/a
on the back	4	n/a	n/a
clasper	3	n/a	n/a
clasper	3	n/a	n/a
clasper	3	n/a	n/a

Shark no.	Sample ID	Mantle weight (mg)	Estimated barnacle size	$\delta^{15}N$ (‰)	%N
3	S3S1B1_EGG	61.97	Medium	10.3	5.9
3	S3S1B2_EGG	20.81	Small	n/a	n/a
3	S3S2B1_EGG	14.39	Small	n/a	n/a
3	S3S2B2_EGG	5.63	Small	n/a	n/a
4	S4S1B1_EGG	94.59	Medium	11.5	7.0
4	S4S1B2_EGG	100.58	Large	9.9	6.6
4	S4S2B1_EGG	113.44	Large	11.4	6.1
4	S4S2B2_EGG	62.46	Medium	10.5	6.2
8	S8S2B1_EGG	87.59	Medium	13.5	6.8
8	S8S2B2_EGG	223.44	Large	n/a	n/a
10	S10S2B1_EGG	30.35	Small	n/a	n/a
11	S11S2B1_EGG	66.62	Medium	10.7	6.1
11	S11S2B2_EGG	15.63	Small	10.1	5.4
12	S12S2B1_EGG	188.90	Large	n/a	n/a
12	S12S2B2_EGG	118.56	Large	n/a	n/a
16	S16S2B1_EGG	138.84	Large	11.4	5.7
16	S16S2B2_EGG	226.67	Large	10.9	5.8
16	S16S2B3_EGG	182.37	Large	10.3	6.7
16	S16S2B4_EGG	159.34	Large	n/a	n/a
17	S17S2B1_EGG	16.33	Small	n/a	n/a
17	S17S2B2_EGG	16.98	Small	n/a	n/a
17	S17S2B3_EGG	4.85	Small	n/a	n/a

$\delta^{13}C$ (‰)	%C	$\delta^{34}S$ (‰)	%S	C/N	Station	Latitude	Longiture	Avg. depth	Shark sex
-21.8	67.0	19.4	0.4	11.4	86	-44.17133	177.43567	929	male
n/a	n/a	n/a	n/a	n/a	86	-44.17133	177.43567	929	male
n/a	n/a	n/a	n/a	n/a	86	-44.17133	177.43567	929	male
n/a	n/a	n/a	n/a	n/a	86	-44.17133	177.43567	929	male
-22.0	68.9	20.1	0.5	9.9	99	-44.3915	174.057	707	male
-22.8	64.1	20.2	0.5	9.8	99	-44.3915	174.057	707	male
-22.4	66.3	20.0	0.5	10.9	99	-44.3915	174.057	707	male
-21.8	71.8	19.9	0.4	11.6	99	-44.3915	174.057	707	male
-21.1	65.7	19.8	0.5	9.7	40	-42.805	183.5485	1026	male
n/a	n/a	n/a	n/a	n/a	40	-42.805	183.5485	1026	male
n/a	n/a	n/a	n/a	n/a	95	-42.61633	180.926	1261	male
-21.6	66.0	17.7	0.5	10.9	100	-44.73317	174.00167	841	male
-22.2	68.8	21.0	0.4	12.8	100	-44.73317	174.00167	841	male
n/a	n/a	n/a	n/a	n/a	100	-44.73317	174.00167	841	female
n/a	n/a	n/a	n/a	n/a	100	-44.73317	174.00167	841	female
-22.6	70.3	19.3	0.3	12.3	66	-44.55583	182.66417	813	female
-22.5	65.0	20.4	0.4	11.3	66	-44.55583	182.66417	813	female
-22.1	62.3	20.2	0.5	9.3	66	-44.55583	182.66417	813	female
n/a	n/a	n/a	n/a	n/a	66	-44.55583	182.66417	813	female
n/a	n/a	n/a	n/a	n/a	66	-44.55583	182.66417	813	male
n/a	n/a	n/a	n/a	n/a	66	-44.55583	182.66417	813	male
n/a	n/a	n/a	n/a	n/a	66	-44.55583	182.66417	813	male

Shark maturity	Shark length (cm)	Shark weight (g)	no. of infected sites
3	39.6	200	2
3	39.6	200	2
3	39.6	200	2
3	39.6	200	2
3	61	1130	2
3	61	1130	2
3	61	1130	2
3	61	1130	2
3	38.1	150	1
3	38.1	150	1
1	52.6	785	1
1 or 2	43	355	1
2 or 2	43	355	1
2	63	1410	1
2	63	1410	1
6	71.1	1950	1
6	71.1	1950	1
6	71.1	1950	1
6	71.1	1950	1
3	62.7	1145	1
3	62.7	1145	1
3	62.7	1145	1

Site 1 - location	Site 1 - no. of barnacles	Site 2 - location	Site 2 - no. of barnacles
dorsal fin	2	pelvic fin	2
dorsal fin	2	pelvic fin	2
dorsal fin	2	pelvic fin	2
dorsal fin	2	pelvic fin	2
tail	2	clapser	2
tail	2	clapser	2
tail	2	clapser	2
tail	2	clapser	2
along the arm fin	2	n/a	n/a
along the arm fin	2	n/a	n/a
clasper	1	n/a	n/a
eye	2	n/a	n/a
eye	2	n/a	n/a
pectoral fin	2	n/a	n/a
pectoral fin	2	n/a	n/a
on the back	4	n/a	n/a
on the back	4	n/a	n/a
on the back	4	n/a	n/a
on the back	4	n/a	n/a
clasper	3	n/a	n/a
clasper	3	n/a	n/a
clasper	3	n/a	n/a

Shark no.	Sample ID	Mantle weight (mg)	Estimated barnacle size	$\delta^{15}N$ (‰)	%N
3	S3S1B1_GIL	61.97	Medium	9.6	13.2
3	S3S1B2_GIL	20.81	Small	10.7	13.1
3	S3S2B1_GIL	14.39	Small	10.3	12.6
3	S3S2B2_GIL	5.63	Small	11.4	12.5
4	S4S1B1_GIL	94.59	Medium	n/a	n/a
4	S4S1B2_GIL	100.58	Large	9.4	11.7
4	S4S2B1_GIL	113.44	Large	11.3	11.8
4	S4S2B2_GIL	62.46	Medium	9.7	12.1
8	S8S2B1_GIL	87.59	Medium	11.7	12.1
8	S8S2B2_GIL	223.44	Large	n/a	n/a
10	S10S2B1_GIL	30.35	Small	14.9	13.2
11	S11S2B1_GIL	66.62	Medium	9.3	11.4
11	S11S2B2_GIL	15.63	Small	9.0	11.8
12	S12S2B1_GIL	188.90	Large	10.4	13.0
12	S12S2B2_GIL	118.56	Large	8.8	10.7
16	S16S2B1_GIL	138.84	Large	10.2	12.8
16	S16S2B2_GIL	226.67	Large	9.7	12.3
16	S16S2B3_GIL	182.37	Large	10.2	14.6
16	S16S2B4_GIL	159.34	Large	9.6	12.4
17	S17S2B1_GIL	16.33	Small	11.7	12.1
17	S17S2B2_GIL	16.98	Small	12.1	13.2
17	S17S2B3_GIL	4.85	Small	n/a	n/a

$\delta^{13}C$ (‰)	%C	$\delta^{34}S$ (‰)	%S	C/N	Station	Latitude	Longiture	Avg. depth	Shark sex
-19.6	46.1	21.1	0.9	3.5	86	-44.2	177.4	929	male
-18.7	41.4	22.3	0.7	3.2	86	-44.2	177.4	929	male
-19.0	43.3	21.5	0.9	3.4	86	-44.2	177.4	929	male
-19.0	40.3	22.3	0.8	3.2	86	-44.2	177.4	929	male
n/a	n/a	n/a	n/a	n/a	99	-44.4	174.1	707	male
-19.6	45.3	21.4	0.9	3.9	99	-44.4	174.1	707	male
-19.5	46.3	20.9	0.8	3.9	99	-44.4	174.1	707	male
-19.5	45.6	21.2	0.9	3.8	99	-44.4	174.1	707	male
-18.0	44.8	21.4	1.1	3.7	40	-42.8	183.5	1026	male
n/a	n/a	n/a	n/a	n/a	40	-42.8	183.5	1026	male
-17.7	42.4	22.6	1.2	3.2	95	-42.6	180.9	1261	male
-18.6	46.3	20.8	0.8	4.0	100	-44.7	174.0	841	male
-18.9	41.8	21.9	0.9	3.6	100	-44.7	174.0	841	male
-18.8	43.3	21.0	0.9	3.3	100	-44.7	174.0	841	female
-18.7	43.9	21.6	0.7	4.1	100	-44.7	174.0	841	female
-18.7	46.8	21.7	0.9	3.7	66	-44.6	182.7	813	female
-18.8	48.2	21.7	0.9	3.9	66	-44.6	182.7	813	female
-18.8	39.5	21.8	1.1	2.7	66	-44.6	182.7	813	female
-18.8	46.4	21.3	0.9	3.7	66	-44.6	182.7	813	female
-18.3	41.8	22.0	0.9	3.5	66	-44.6	182.7	813	male
-18.2	43.4	22.5	1.1	3.3	66	-44.6	182.7	813	male
n/a	n/a	n/a	n/a	n/a	66	-44.6	182.7	813	male

Shark maturity	Shark length (cm)	Shark weight (g)	no. of infected sites
3	39.6	200	2
3	39.6	200	2
3	39.6	200	2
3	39.6	200	2
3	61	1130	2
3	61	1130	2
3	61	1130	2
3	61	1130	2
3	38.1	150	1
3	38.1	150	1
1	52.6	785	1
1 or 2	43	355	1
2 or 2	43	355	1
2	63	1410	1
2	63	1410	1
6	71.1	1950	1
6	71.1	1950	1
6	71.1	1950	1
6	71.1	1950	1
3	62.7	1145	1
3	62.7	1145	1
3	62.7	1145	1

Site 1 - location	Site 1 - no. of barnacles	Site 2 - location	Site 2 - no. of barnacles
dorsal fin	2	pelvic fin	2
dorsal fin	2	pelvic fin	2
dorsal fin	2	pelvic fin	2
dorsal fin	2	pelvic fin	2
tail	2	clapser	2
tail	2	clapser	2
tail	2	clapser	2
tail	2	clapser	2
along the arm fin	2	n/a	n/a
along the arm fin	2	n/a	n/a
clasper	1	n/a	n/a
eye	2	n/a	n/a
eye	2	n/a	n/a
pectoral fin	2	n/a	n/a
pectoral fin	2	n/a	n/a
on the back	4	n/a	n/a
on the back	4	n/a	n/a
on the back	4	n/a	n/a
on the back	4	n/a	n/a
clasper	3	n/a	n/a
clasper	3	n/a	n/a
clasper	3	n/a	n/a